



# Multi-fidelity machine learning based uncertainty quantification of progressive damage in composite laminates through optimal data fusion

R.S. Chahar<sup>a,1</sup>, T. Mukhopadhyay<sup>b,\*,1</sup>

<sup>a</sup> Department of Aerospace Engineering, Indian Institute of Technology Kanpur, Kanpur, India

<sup>b</sup> School of Engineering, University of Southampton, Southampton, UK

## ARTICLE INFO

### Keywords:

Stochastic progressive damage  
Gaussian process  
Multi-fidelity surrogates  
Continuum damage mechanics  
Uncertainty quantification of composites  
Sensitivity analysis of composites

## ABSTRACT

Recently machine learning (ML) based approaches have gained significant attention in dealing with computationally intensive analyses such as uncertainty quantification of composite laminates. However, high-fidelity ML model construction is computationally demanding for such high-dimensional problems due to the required large amount of high-fidelity training data. We propose to address this issue effectively through multi-fidelity ML based surrogates which can use a training dataset consisting of optimally distributed high- and low-fidelity simulations. For forming multi-fidelity surrogates of progressive damage in composite laminates, we combine low-fidelity finite element analysis data obtained using Matzenmiller damage model with Hasin failure criteria and high-fidelity finite element analysis data obtained using three-dimensional continuum damage mechanics based model with P Linde's failure criteria. It is shown that there is a significant computational advantage to using the multi-fidelity surrogate approach as compared to conventional single-fidelity surrogates. Such computational advantage through optimal data fusion without compromising accuracy becomes crucial for the subsequent data-driven uncertainty quantification and sensitivity analysis of composites involving thousands of realizations. Ply orientations come out to be the most sensitive parameters to matrix damage, fibre damage and reaction force in composite laminates. The degree of uncertainty in the output quantities depend on the input-level stochastic variations. For example, a combined stochastic variation of  $\pm 10\%$  in material properties and  $\pm 10^\circ$  in ply orientations lead to 1.85%, 16.98% and 11.24% coefficient of variation in the matrix damage, fibre damage and reaction force respectively. In general, the numerical results obtained based on the efficient data-driven approach strongly suggest that source-uncertainty of composites significantly influences the progressive damage evolution and global mechanical behaviour, leading to the realization of the importance of adopting an inclusive analysis framework considering such inevitable random variabilities.

## 1. Introduction

Analysis of composite laminates has been challenging not only due to the occurrence of multiple failure and damage mechanisms but also due to uncertainty in the material and geometric properties (Sriramula and Chrystanthopoulos, 2009; Tornabene et al., 2018; Mukhopadhyay et al., 2018; Mandal and Chakrabarti, 2018; Pagani et al., 2023; Sharma et al., 2022a). Various failure criteria and damage models have been used in the past to predict the damage and failure in composite laminates (Hinton et al., 2002; Gao et al., 2020). Continuum damage mechanics-based models are one of the most widely used progressive damage models for simulating the failure mechanisms in composite laminates (Matzenmiller et al., 1995; Maimí et al., 2007; Ghannadpour et al., 2018; Ansari and Chakrabarti, 2016). The progressive damage models incorporate damage initiation criteria for predicting the onset of damage and damage evolution criteria for damage progression.

The focus of this article is to propose an efficient Gaussian process-based multi-fidelity surrogate modelling approach for quantifying the uncertainty associated with progressive damage in composite laminates. The developed multi-fidelity surrogate models would further be exploited for variance-based global sensitivity analysis to investigate the relative influence of input parameters on laminate responses and damage propagation behaviour.

Over the last decade, surrogate-based (Sharma et al., 2022b) uncertainty quantification has been used increasingly to quantify the uncertain global responses in the composite laminates considering uncertainty in the material and geometric properties. Dey et al. (2016b) applied a surrogate approach to perform stochastic analysis of the frequency response of composite laminates considering uncertainty in elastic modulus, mass density and ply orientation angle. A comparison between the predictions of General High Dimensional Model

\* Corresponding author.

E-mail address: [t.mukhopadhyay@soton.ac.uk](mailto:t.mukhopadhyay@soton.ac.uk) (T. Mukhopadhyay).

<sup>1</sup> Both the authors have contributed equally.

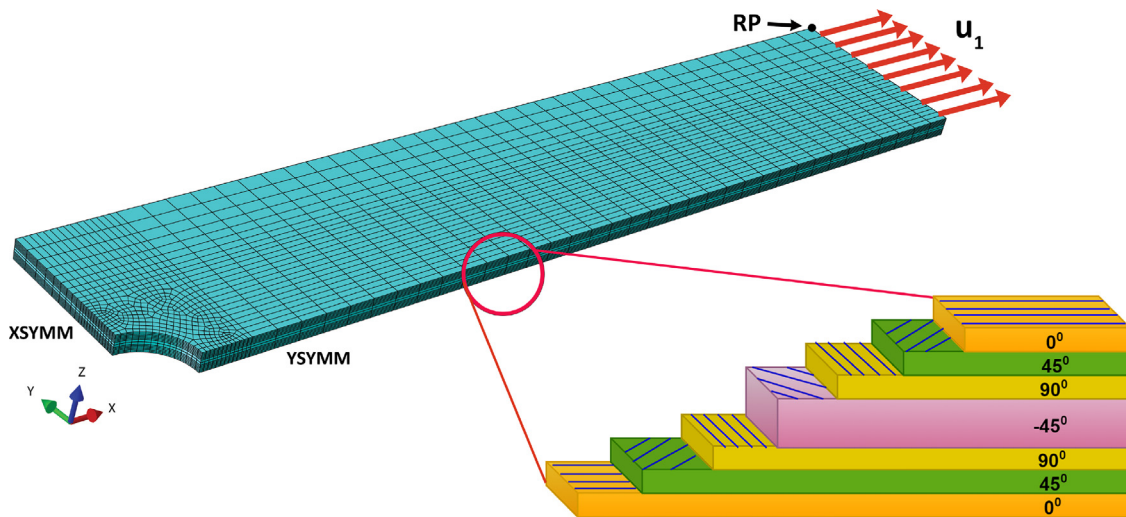


**Fig. 1. Geometry and boundary conditions of the notched composite laminate under investigation.** AS4/PEEK  $([0/45/90/-45])_{2,5}$  composite layup is considered having width = 20 mm, length = 100 mm and a circular hole of 5 mm diameter at the centre. Considering the symmetry, only one-quarter of the composite is modelled and displacement controlled load is applied at the reference point (RP).

Representative (GHDMR) and commercial finite element (FE) software ANSYS was done for the frequency response of the composite laminate. Naskar et al. (2018) used a random field-based surrogate approach to quantify the effect of spatial variation in micromechanical properties on the frequency response of composite laminates. Surrogate and machine learning based approaches have been widely integrated in the uncertainty quantification (probabilistic and non-probabilistic) of composite structures concerning dynamic analyses including augmentation of lower order theories (Vaishali et al., 2023; Naskar et al., 2019; Vaishali et al., 2021; Dey et al., 2016a; Mukhopadhyay et al., 2021). Of late stochastic failure analysis of composite structures have been reported in the literature (Bhowmik et al., 2022; Karsh et al., 2018). A comprehensive account of surrogate-based approaches for stochastic dynamic and stability analysis of laminated composites is presented in the recent monograph by Dey et al. (2018). The rationale behind involving surrogate models in uncertainty quantification is that a Monte Carlo simulation-based approach for complete probabilistic characterization requires thousands of function evaluations (i.e. same number of expensive FE simulations), while a computationally efficient surrogate can effectively replace the requirement of carrying out a large number of such FE simulations.

Propagation of the uncertainty is essential to capture the nonlinear constitutive behaviour and understand the failure mechanisms accurately (Tao et al., 2020). Several works have tried to use an artificial neural network (ANN) (Hosseinpour et al., 2023) to understand the constitutive behaviour (stress-strain and load-displacement curves) of composite laminates (Yan et al., 2020; Liu et al., 2020; Tao et al., 2021). Bostanabad et al. (2018) employed a Gaussian process-based surrogate approach to quantify the load-displacement response and stresses in woven fibre composites due to spatial variation in fibre misalignment angle, fibre volume fraction and yarn angle. Surrogate models have been utilized to carry out global sensitivity analysis (Thapa et al., 2021; Balokas et al., 2021b) for understanding the effect of variation in input parameters on strength and ultimate failure of composite laminates.

The finite element model which has a sufficient amount of accuracy but normally requires a high amount of computational cost can be called a high-fidelity (HF) model whereas a model which requires less amount of computational cost but is less accurate than the HF model can be called a low-fidelity (LF) model. It is expected that a surrogate model formed using HF training data would predict more accurately (with respect to the ground truth) compared to that formed using LF training data. Multi-fidelity (MF) modelling (Forrester et al., 2007; Yoo et al., 2021; Balokas et al., 2021a) makes a trade-off between

computationally expensive high-fidelity models and computationally cheaper low-fidelity models for making reasonably accurate predictions. The adoption of such MF modelling can reduce the computational burden for training data generation in a surrogate-based approach of uncertainty quantification by involving a high number of cheap low-fidelity data. West IV and Phillips (2020) used a multi-fidelity approach to quantify the uncertainty in drag and ground noise of the commercial supersonic aircraft reducing 50% and 70% computational cost respectively. Guo et al. (2020) applied a multi-fidelity surrogate approach to optimize the buckling load of variable stiffness composite cylinders considering low-fidelity FE models with a coarse mesh and high-fidelity FE models with a fine mesh. A similar approach was applied by Krishnan and Ganguli (2021) for analysing the dynamic response of composite beams considering Euler-Bernoulli beam FE model as the LF model and Timoshenko beam FE model as the HF model. Balokas et al. (2021a) developed a variable-fidelity approach for strength analysis of braided composites based on LF USDFLD model and HF UMAT model considering the micromechanical properties. Tian et al. (2021), Xu et al. (2023) used a transfer learning-based surrogate approach to solve the variable stiffness composite shell problem and later visualized the full-field strength information of the stiffened plate structure. Lin et al. (2022) developed sequential sampling-based multi-fidelity surrogate modelling for robust design optimization, wherein an extended upper confidence boundary (EUCB) function was maximized to determine the sampling locations of the sequential samples and surrogate fidelity levels.

There has been a common consensus to reduce computational expenses in generating the training dataset for machine learning model formation. Solution of complex finite element problems such as progressive damage evolution and constitutive modelling of composites, which normally involves a large number of input parameters, incur huge computational costs as each finite element simulation is exorbitantly time-consuming. The studies on prediction of strength and progressive damage for notched composite laminates based on multi-fidelity surrogate approach considering material and geometric uncertainty are relatively scarce in literature. The objective of this work is to reduce the computational burden in uncertainty quantification of progressive damage and evaluation of stochastic failure strength based on multi-fidelity surrogate modelling approach.

We would establish the HF and LF models for progressive damage analysis of composite laminates (refer to Fig. 1) in this paper based on accuracy in prediction with respect to experimental data and computational time (Maa and Cheng, 2002). As shown in the following sections,

Abaqus built-in model would be taken as a LF FEA model, while the three-dimensional continuum damage mechanics-based damage model coupled with P Linde's failure criteria, implemented in user subroutine UMAT, would be considered as a HF FEA model. Each HF finite element simulation for accurate progressive damage analysis of composite laminates being computationally very expensive, it is imperative to develop MF surrogate approaches for maximizing the computational savings in machine learning model formation for subsequent uncertainty quantification. A Gaussian process-based machine learning algorithm would be developed here in conjunction with finite element simulations for the multi-fidelity surrogate modelling to quantify the uncertainty in matrix damage, fibre damage and delamination along with the constitutive behaviour of composite laminates considering stochasticity in material properties and fibre orientation. The MF surrogate approach would be further exploited to perform a variance-based global sensitivity analysis to investigate the relative influence of input parameters on the global mechanical behaviour of composite laminates. The hybrid multi-fidelity machine learning models can be regarded here as the most efficient surrogate of the occurrence of progressive damage in composite laminates that unify high and low fidelity damage models through optimal data fusion.

The novelty and impact of this article while addressing the above-identified research gaps would be two-fold: (1) quantifying the uncertainty associated with progressive failure of composites, leading to complete probabilistic descriptions along with sensitivity analysis, (2) developing the multi-fidelity ML based approach in conjunction with finite element simulations for efficient progressive damage analysis through optimal data fusion. Note that such multi-fidelity data fusion is attempted here for the first time in the high dimensional stochastic design space of laminated composites for subsequent uncertainty quantification. Thus the primary contribution of this article is envisaged to lie in coupling multi-fidelity machine learning models with optimal fusion of two different finite element based damage models of variable fidelity (Matzenmiller damage model with Hashin failure criteria and three-dimensional continuum mechanics based damage model with P Linde's failure criteria) for most efficient stochastic analysis of the progressive damage in composite laminates.

The remainder of the article is organized as follows: Section 2 describes the modelling of deterministic failure for the low-fidelity FE approach (FE model 1) and high-fidelity FE approach (FE model 2); Section 3 explains the multi-fidelity surrogate modelling along with subsequent uncertainty quantification; the global sensitivity analysis is described in Section 4; Section 5 discusses numerical results for notched composite laminates loaded under uniaxial tension; Section 6 presents concluding remarks.

## 2. Deterministic progressive failure modelling

As discussed in the preceding section, two different finite element models are adopted here for the prediction of the composite laminate constitutive behaviour. Abaqus built-in model is taken as a LF FEA model (FE model 1), while the three-dimensional continuum damage mechanics-based damage model coupled with P Linde's failure criteria, implemented in user subroutine UMAT, is considered as a HF FEA model (FE model 2). Brief descriptions of these two models are provided in this section.

### 2.1. Modelling of fibre and matrix damage: FE model 1 (LF model)

In FE model 1, a damage model proposed by Matzenmiller et al. (1995) with Hashin failure criteria (Hashin, 1980) is used for the prediction of the initiation of fibre and matrix damage. Hashin 2D failure criteria is an in-built failure criterion in commercial finite element code Abaqus (Smith, 2009). It uses four failure modes for the damage initiation:

Fibre Tension ( $\hat{\sigma}_{11} \geq 0$ ) :

$$F_{f_t}(\hat{\sigma}_{11}, \hat{\sigma}_{12}) = \left(\frac{\hat{\sigma}_{11}}{X_T}\right)^2 + \hat{\alpha} \left(\frac{\hat{\sigma}_{12}}{S_L}\right)^2 = 1 \quad (1)$$

Fibre Compression ( $\hat{\sigma}_{11} < 0$ ) :

$$F_{f_c}(\hat{\sigma}_{11}) = \left(\frac{\hat{\sigma}_{11}}{X_C}\right)^2 = 1 \quad (2)$$

Matrix Tension ( $\hat{\sigma}_{22} \geq 0$ ) :

$$F_{m_t}(\hat{\sigma}_{22}, \hat{\sigma}_{12}) = \left(\frac{\hat{\sigma}_{22}}{Y_T}\right)^2 + \left(\frac{\hat{\sigma}_{12}}{S_L}\right)^2 = 1 \quad (3)$$

Matrix Compression ( $\hat{\sigma}_{22} < 0$ ) :

$$F_{m_c}(\hat{\sigma}_{22}, \hat{\sigma}_{12}) = \left(\frac{\hat{\sigma}_{22}}{2S_T}\right)^2 + \left[\left(\frac{Y_C}{2S_T}\right)^2 - 1\right] \left(\frac{\hat{\sigma}_{22}}{Y_C}\right) + \left(\frac{\hat{\sigma}_{12}}{S_L}\right)^2 = 1 \quad (4)$$

In the above Eqs. (1)–(4),  $\hat{\sigma}_{ij}(i, j = 1, 2)$  are effective stress tensor components while  $X_T$ ,  $X_C$ ,  $Y_T$ ,  $Y_C$  denote longitudinal tensile strength, longitudinal compressive strength, transverse tensile strength and transverse compressive strength, respectively.  $S_L$ ,  $S_T$  denote in-plane and transverse shear strengths respectively.  $F_{f_t}$ ,  $F_{f_c}$ ,  $F_{m_t}$  and  $F_{m_c}$  denote the initiation of the damage in the given failure modes. The damaged elasticity matrix (Lapczyk and Hurtado, 2007) is obtained using the model proposed by Matzenmiller et al. (1995).

$$C_d = \frac{1}{\bar{D}} \begin{bmatrix} (1-D_f)E_1 & (1-D_f)(1-D_m)v_{21}E_1 & 0 \\ (1-D_f)(1-D_m)v_{12}E_2 & (1-D_m)E_2 & 0 \\ 0 & 0 & \bar{D}(1-D_s)G_{12} \end{bmatrix} \quad (5)$$

where  $\bar{D} = 1 - (1-D_f)(1-D_m)v_{21}v_{21}$ , and the parameters  $D_f$ ,  $D_m$  and  $D_s$  are fibre damage, matrix damage and shear damage variables respectively.  $E_1$ ,  $E_2$  and  $G_{12}$  are material moduli and  $v_{12}$ ,  $v_{21}$  are Poisson's ratios of undamaged material.  $D_s = 1 - (1-D_f)(1-D_m)(1-D_m)$ , while the parameters  $D_{f_t}$ ,  $D_{f_c}$ ,  $D_{m_t}$  and  $D_{m_c}$  are used to denote fibre and matrix damage variables in tension and compression ('t' denotes tension and 'c' denotes compression) as explained in Lapczyk and Hurtado (2007).

Once a damage initiation has occurred, further material degradation follows the damage evolution law. A damage evolution law based on fracture energy is used with the assumption of linear material softening. Each failure mode  $K$  is governed by the following damage variable

$$d_K = \frac{\delta_{K,eq}^f (\delta_{K,eq}^f - \delta_{K,eq}^0)}{\delta_{K,eq}^f (\delta_{K,eq}^f - \delta_{K,eq}^0)} \quad K \in \{f_t, f_c, m_t, m_c\} \quad (6)$$

where,  $\delta_{K,eq}^0$  denotes equivalent displacement at which the damage onset happens, and  $\delta_{K,eq}^f$  denotes equivalent displacement at which full degradation of material happens.

### 2.2. Modelling of fibre and matrix damage: FE model 2 (HF model)

In this model, failure criteria suggested by Linde et al. (2004) is incorporated in the UMAT user subroutine to predict the fibre and the matrix damage. The failure modes used for the initiation of damage are as follows

$$f_f(\epsilon_{11}) = \sqrt{\frac{\hat{\epsilon}_{11}^t}{\hat{\epsilon}_{11}^c} (\epsilon_{11})^2 + \left[\hat{\epsilon}_{11}^t - \frac{(\hat{\epsilon}_{11}^t)^2}{\hat{\epsilon}_{11}^c}\right] \epsilon_{11}} > \hat{\epsilon}_{11}^t \quad (7)$$

$$f_m(\epsilon_{22}, \epsilon_{12}) = \sqrt{\frac{\hat{\epsilon}_{22}^t}{\hat{\epsilon}_{22}^c} (\epsilon_{22})^2 + \left[\hat{\epsilon}_{22}^t - \frac{(\hat{\epsilon}_{22}^t)^2}{\hat{\epsilon}_{22}^c}\right] \epsilon_{22} + \left(\frac{\hat{\epsilon}_{12}^t}{\hat{\epsilon}_{12}^c}\right)^2 (\epsilon_{12})^2} > \hat{\epsilon}_{22}^t \quad (8)$$

where  $\hat{\epsilon}_{11}^t$ ,  $\hat{\epsilon}_{11}^c$ ,  $\hat{\epsilon}_{22}^t$ ,  $\hat{\epsilon}_{22}^c$  are the failure strain in the fibre direction in tension, failure strain in the fibre direction in compression, failure strain perpendicular to the fibre direction in tension and failure strain

**Table 1**  
Material properties of AS4/PEEK composite (Maa and Cheng, 2002; Chen et al., 2012).

Parameter	Value
Longitudinal elastic modulus ( $E_1$ )	139 000 MPa
Transverse elastic modulus ( $E_2$ )	10 200 MPa
In-plane shear modulus ( $G_{12}$ )	5900 MPa
Transverse shear modulus ( $G_{23}$ )	3700 MPa
In-plane Poisson's ratio ( $\nu_{12}$ )	0.32
Transverse Poisson's ratio ( $\nu_{23}$ )	0.45
Longitudinal tensile strength ( $X_T$ )	2023 MPa
Longitudinal compressive strength ( $X_C$ )	1234 MPa
Transverse tensile strength ( $Y_T$ )	92.7 MPa
Transverse compressive strength ( $Y_C$ )	176 MPa
In-plane shear strength ( $S_{12}$ )	82.6 MPa
Matrix fracture energy in tension ( $G_m$ )	5.6 N/mm
Fibre fracture energy in tension ( $G_{ft}$ )	128 N/mm

**Table 2**  
Material properties of Adhesive layers (Chen et al., 2014).

$K_{mm}^0 = K_{ss}^0 = K_{tt}^0$	$\sigma_n^0$	$\tau_s^0$	$\tau_t^0$	$G_{Ic}$	$G_{IIc}$	$G_{IIIc}$
$10^6$ N/mm <sup>3</sup>	80 MPa	100 MPa	100 MPa	0.969 N/mm	1.719 N/mm	2.01 N/mm

**Table 3**  
Comparison of failure loads and percentage error between the present FEA models and the experimental data for AS4/PEEK ( $[0^\circ/45^\circ/90^\circ/-45^\circ]_{2S}$ ) composite layup.

Failure load (kN)			Error (%)	
Present (Abaqus built-in)	Present (UMAT)	Maa and Cheng (Experimental)	Present (Abaqus built-in)	Present (UMAT)
19.323	16.149	15.31	26.2116	5.48

**Table 4**  
Comparison of computational costs of the present finite element analysis (FEA) models for AS4/PEEK ( $[0^\circ/45^\circ/90^\circ/-45^\circ]_{2S}$ ) composite layup till the final failure.

FEA model	CPU time (s)	Wallclock time (s)
Abaqus built-in	2220	332
UMAT	6453	1036

perpendicular to the fibre direction in compression respectively. Failure occurs when  $f_f$  and  $f_m$  exceeds  $\hat{\epsilon}_{11}^f$  and  $\hat{\epsilon}_{22}^f$  respectively.

After the damage initiation, further material degradation follows the damage evolution law

$$d_f = 1 - \frac{\hat{\epsilon}_{11}^f}{f_f} e^{(-C_{11}\hat{\epsilon}_{11}^f (f_f - \hat{\epsilon}_{11}^f) L^c / G_f)} \quad (9)$$

$$d_m = 1 - \frac{\hat{\epsilon}_{22}^f}{f_m} e^{(-C_{22}\hat{\epsilon}_{22}^f (f_m - \hat{\epsilon}_{22}^f) L^c / G_m)} \quad (10)$$

The damaged elasticity matrix (Linde et al., 2004) is obtained as follows

$$C_d = \begin{bmatrix} (1 - D_f)C_{11} & (1 - D_f)(1 - D_m)C_{12} & (1 - D_f)C_{13} & 0 & 0 & 0 \\ & (1 - D_m)C_{22} & (1 - D_m)C_{23} & 0 & 0 & 0 \\ & & C_{33} & 0 & 0 & 0 \\ & & & (1 - D_f)(1 - D_m)C_{44} & 0 & 0 \\ & \text{symm} & & & C_{55} & 0 \\ & & & & & C_{66} \end{bmatrix} \quad (11)$$

### 2.3. Delamination modelling

In both the FE models (FE model 1 and FE model 2), cohesive zone method which has been implemented in Abaqus FEA (Smith, 2009), is used to model the delamination damage. Before the initiation of delamination, traction–separation relation is assumed as linearly elastic to describe the interaction between adjacent surfaces.

$$\begin{Bmatrix} \sigma_n \\ \tau_s \\ \tau_t \end{Bmatrix} = \begin{bmatrix} K_{mm}^0 & 0 & 0 \\ 0 & K_{ss}^0 & 0 \\ 0 & 0 & K_{tt}^0 \end{bmatrix} \begin{Bmatrix} \delta_n \\ \delta_s \\ \delta_t \end{Bmatrix} \quad (12)$$

where,  $\sigma_n$ ,  $\tau_s$  and  $\tau_t$  are nominal traction vectors.  $K_{mm}^0$ ,  $K_{ss}^0$  and  $K_{tt}^0$  are penalty stiffness coefficients and  $\delta_n$ ,  $\delta_s$  and  $\delta_t$  are relative displacements (Sharma et al., 2017). The quadratic stress criterion is used for the onset of delamination (Chen et al., 2014).

$$\left( \frac{\langle \sigma_n \rangle}{\sigma_n^0} \right)^2 + \left( \frac{\tau_s}{\tau_s^0} \right)^2 + \left( \frac{\tau_t}{\tau_t^0} \right)^2 = 1 \quad (13)$$

where  $\langle \cdot \rangle$  represents Macaulay bracket and  $\sigma_n^0$ ,  $\tau_s^0$  and  $\tau_t^0$  are the interface strengths in mode I, mode II and mode III, respectively.

Once the damage initiation criterion of the delamination is satisfied, delamination propagates as per power-law criterion (Chen et al., 2014).

$$\left( \frac{G_I}{G_{Ic}} \right)^{\tilde{\gamma}} + \left( \frac{G_{II}}{G_{IIc}} \right)^{\tilde{\gamma}} + \left( \frac{G_{III}}{G_{IIIc}} \right)^{\tilde{\gamma}} = 1 \quad (14)$$

where,  $G_{Ic}$ ,  $G_{IIc}$  and  $G_{IIIc}$  are interfacial critical fracture energies in modes I, II and III respectively. In this work,  $\tilde{\gamma} = 1$  is taken in Eq. (14). Such selection suits well for the prediction of complete delamination in AS4/PEEK thermoplastic composites (Chen et al., 2014; Camanho et al., 2003). AS4/PEEK composite lamina and adhesive layer material properties are given in Table 1 and Table 2 respectively.

### 2.4. Remarks on multi-fidelity

A mesh convergence study of the finite element models (Abaqus built-in and UMAT model) is presented in Fig. 3(A–B). Note that the behaviour of the entire constitutive curve along with the failure point is of critical significance here. Based on the converged results, it is noted from Fig. 3(C) that UMAT FE model predictions are closer to experimental data than Abaqus built-in FE model, making the UMAT model more accurate than Abaqus built-in model. The percentage error between the two models is given in Table 3. The UMAT model becomes slow for the applied displacements close to failure. This is due to convergence rate at higher applied loads. The comparison of computational costs of UMAT model and Abaqus-built-in model are presented in Table 4. Such results justify our consideration of the UMAT FE model as the high-fidelity model (with more computational cost) and the Abaqus built-in model as a low-fidelity model (with lesser computational cost) for subsequent multi-fidelity machine learning

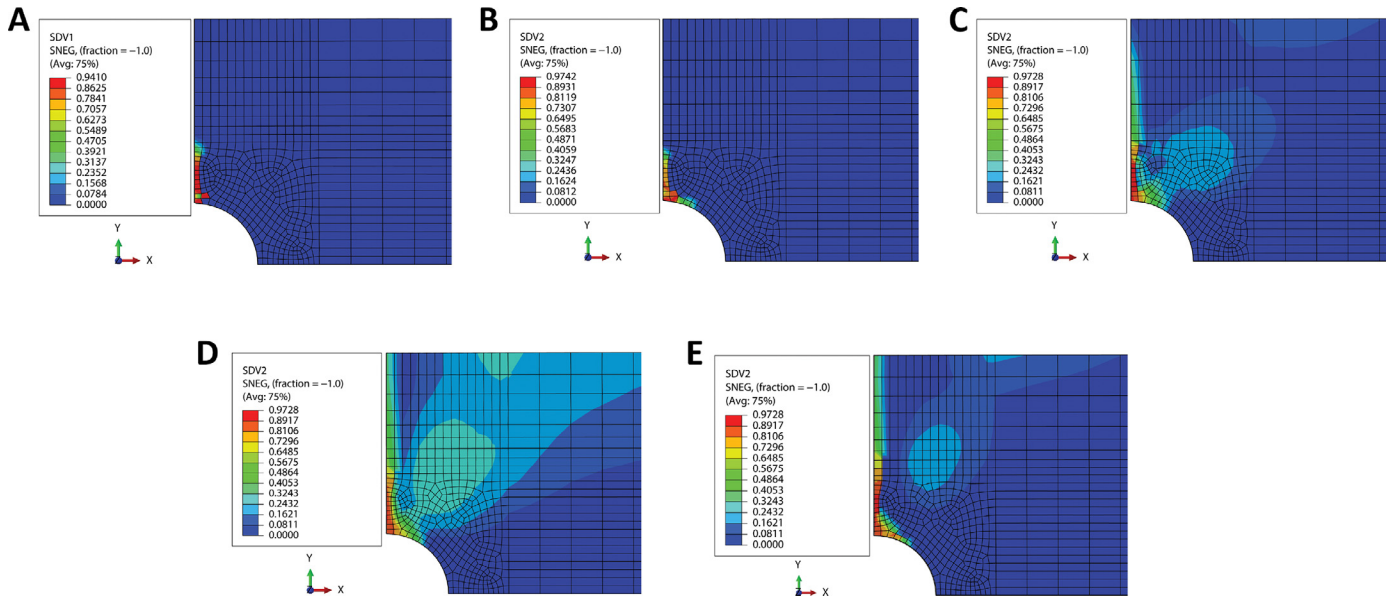


Fig. 2. Contour plots of fibre and matrix damage (A) Fibre damage in 0° ply, (B) Matrix damage in 0° ply, (C-E) Matrix damages in 45°, 90° and -45° plies respectively.

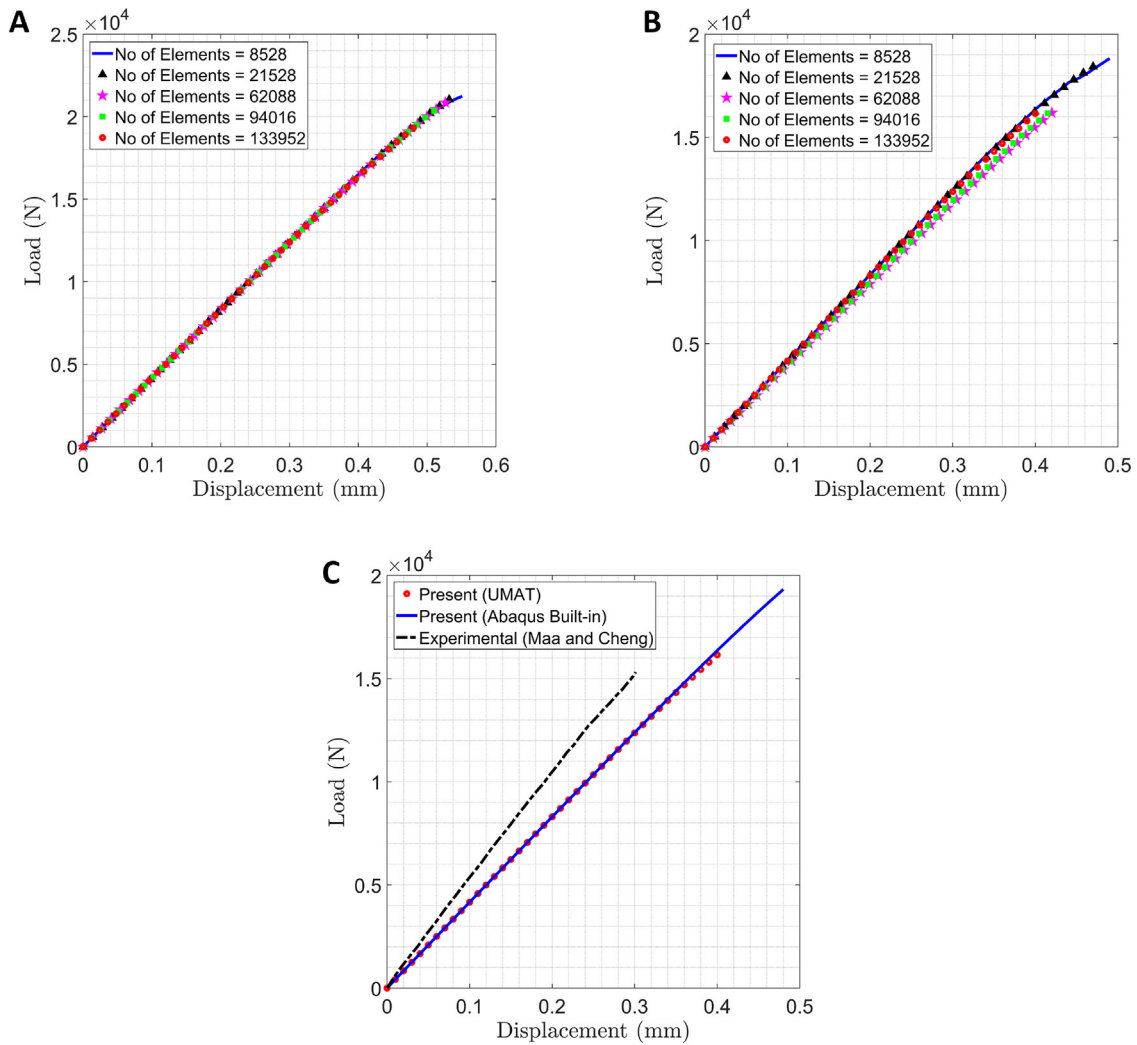


Fig. 3. Load-displacement curves of the notched composite laminate. (A) Mesh sensitivity of load displacement curves for Abaqus built-in model. (B) Mesh sensitivity of load displacement curves for UMAT model. (C) Comparison of predicted load-displacement curves of LF and HF finite element analysis (FEA) simulations with experimental data of Maa and Cheng (2002). The LF FEA simulation is based on Hashin failure criteria (Abaqus built-in) and the HF FEA simulation is based on P Linde's failure criteria (UMAT).

model formation. In this context, it may further be noted that the approach of coupling low and high-fidelity damage models through machine learning is generic in nature. Other low and high-fidelity models can be optimally integrated following a similar framework based on the problem under consideration.

### 3. Gaussian process algorithm based multi-fidelity stochastic analysis

This section presents a multi-fidelity surrogate approach based on Gaussian process, coupled with the finite element simulation presented in the preceding section, to quantify the uncertainty in progressive damage of composite laminates. Assuming that  $v_1(x)$  and  $v_2(x)$  are two independently chosen Gaussian processes having mean as zero and covariance functions,  $c_1$  and  $c_2$  respectively. It can be written in the mathematical form as,

$$v_1(x) \sim GP(0, c_1(x, x'; \Omega_1)) \quad , \quad v_2(x) \sim GP(0, c_2(x, x'; \Omega_2)) \quad (15)$$

The covariance functions  $c_1$  and  $c_2$  are squared exponential functions of the form

$$c(x, x'; \Omega) = \alpha^2 \exp \left( -\frac{1}{2} \sum_{p=1}^P \frac{(x_p - x'_p)^2}{\beta_p^2} \right) \quad (16)$$

where  $\Omega = (\alpha, \beta)$  are the hyper-parameters.

We model the low-fidelity function by  $f_l(x) = v_1(x)$  and high-fidelity function by  $f_h(x) = \rho v_1(x) + v_2(x)$ . This will result in the following expression (Raissi and Karniadakis, 2016),

$$\begin{bmatrix} f_l(x) \\ f_h(x) \end{bmatrix} \sim GP \left( 0, \begin{bmatrix} c_{ll}(x, x'; \Omega_1) & c_{lh}(x, x'; \Omega_1, \rho) \\ c_{hl}(x, x'; \Omega_1, \rho) & c_{hh}(x, x'; \Omega_1, \Omega_2, \rho) \end{bmatrix} \right), \quad (17)$$

where

$$\begin{aligned} c_{ll}(x, x'; \Omega_1) &= c_1(x, x'; \Omega_1), \\ c_{lh}(x, x'; \Omega_1, \rho) &= c_{lh}(x, x'; \Omega_1, \rho) = \rho c_1(x, x'; \Omega_1), \\ c_{hh}(x, x'; \Omega_1, \Omega_2, \rho) &= \rho^2 c_1(x, x'; \Omega_1) + c_2(x, x'; \Omega_2) \end{aligned}$$

#### 3.1. Training

Given the training data  $\{x_l, y_l\}$  and  $\{x_h, y_h\}$ , we assume that

$$y_l = f_l(x_l) + \epsilon_l, \quad \epsilon_l \sim \mathcal{N}(0, \sigma_l^2 \mathbf{I}),$$

and

$$y_h = f_h(x_h) + \epsilon_h, \quad \epsilon_h \sim \mathcal{N}(0, \sigma_h^2 \mathbf{I})$$

Consequently, we obtain

$$\mathbf{y} \sim \mathcal{N}(\mathbf{0}, \mathbf{C}), \quad (18)$$

where

$$\mathbf{y} = \begin{bmatrix} y_l \\ y_h \end{bmatrix}$$

and

$$\mathbf{C} = \begin{bmatrix} c_{ll}(x_l, x_l; \Omega_1) + \sigma_l^2 \mathbf{I} & c_{lh}(x_l, x_h; \Omega_1, \rho) \\ c_{hl}(x_h, x_l; \Omega_1, \rho) & c_{hh}(x_h, x_h; \Omega_1, \Omega_2, \rho) + \sigma_h^2 \mathbf{I} \end{bmatrix}$$

The hyper-parameters  $\Omega_1, \Omega_2, \rho$  and the noise variance parameters  $\sigma_l^2, \sigma_h^2$  are trained by minimization of the negative log marginal likelihood (Raissi et al., 2017), which can be written as

$$\mathcal{L}(\Omega_1, \Omega_2, \rho) = \frac{1}{2} \log |\mathbf{C}| + \frac{N}{2} \log(2\pi) + \frac{1}{2} \mathbf{y}^T \mathbf{C}^{-1} \mathbf{y} \quad (19)$$

#### 3.2. Prediction

After training the model, the prediction is done at a new test point  $x^*$  by writing the joint distribution

$$\begin{bmatrix} f_h(x^*) \\ \mathbf{y} \end{bmatrix} \sim \mathcal{N} \left( 0, \begin{bmatrix} c_{hh}(x^*, x^*; \Omega_1, \Omega_2, \rho) & \mathbf{q}^T \\ \mathbf{q} & \mathbf{C} \end{bmatrix} \right), \quad (20)$$

where

$$\mathbf{q}^T = [c_{hl}(x^*, x_l; \Omega_1, \rho) \quad c_{hh}(x^*, x_h; \Omega_1, \Omega_2, \rho)]$$

Then conditional distribution can be used to make the predictions

$$f_h(x^*) | \mathbf{y} \sim \mathcal{N}(\mathbf{q}^T \mathbf{C}^{-1} \mathbf{y}, c_{hh}(x^*, x^*) - \mathbf{q}^T \mathbf{C}^{-1} \mathbf{q}) \quad (21)$$

#### 3.3. Stochastic analysis of composite laminates

The stochasticity in elastic properties ( $E_1, E_2, G_{12}, G_{23}, \nu_{12}, \nu_{23}$ ), failure properties ( $X_T, Y_T, S_{12}, G_{m1}, G_{f1}$ ), ply orientations ( $\theta_1, \theta_2, \theta_3$ ) and applied displacement ( $u_1$ ) is considered to study the effect of source-uncertainty in the responses of composite laminates. Considering the practical implementation of the fibre orientations,  $0^\circ, 45^\circ$  and  $90^\circ$  plies (only unique fibre orientation angles) are considered as three variables for defining uncertainty in all 16 plies of  $([0/45/90/-45])_{2S}$  laminated composite layup. Only magnitude of  $45^\circ$  is taken as a variable for defining the uncertainty in  $45^\circ$  and  $-45^\circ$  plies. Variation in the material properties and displacement is taken as  $\pm 10\%$  while variation in the ply orientations is taken as  $\pm 10^\circ$  with respect to nominal values (as per common industry standards). The following cases are considered for performing Monte Carlo simulations based on multi-fidelity surrogates, keeping the nominal applied displacement at 0.3 mm:

(1) Only varying elastic properties ( $E_1, E_2, G_{12}, G_{23}, \nu_{12}, \nu_{23}$ ) which can be written as:

$$\begin{aligned} &g^I \{E_1(\omega), E_2(\omega), G_{12}(\omega), G_{23}(\omega), \nu_{12}(\omega), \nu_{23}(\omega)\} \\ &= \left\{ \begin{array}{l} \psi^1(E_{1(1)} \dots E_{1(l)}), \psi^2(E_{2(1)} \dots E_{2(l)}), \psi^3(G_{12(1)} \dots G_{12(l)}), \\ \psi^4(G_{23(1)} \dots G_{23(l)}), \\ \psi^5(\nu_{12(1)} \dots \nu_{12(l)}), \psi^6(\nu_{23(1)} \dots \nu_{23(l)}) \end{array} \right\} \end{aligned}$$

(2) Only varying failure properties ( $X_T, Y_T, S_{12}, G_{m1}, G_{f1}$ ) which can be written as:

$$\begin{aligned} &g^{II} \{X_T(\omega), Y_T(\omega), S_{12}(\omega), G_{m1}(\omega), G_{f1}(\omega)\} \\ &= \left\{ \begin{array}{l} \psi^1(X_{T(1)} \dots X_{T(l)}), \psi^2(Y_{T(1)} \dots Y_{T(l)}), \psi^3(S_{12(1)} \dots S_{12(l)}), \\ \psi^4(G_{m1(1)} \dots G_{m1(l)}), \psi^5(G_{f1(1)} \dots G_{f1(l)}) \end{array} \right\} \end{aligned}$$

(3) Only varying geometric properties ( $\theta_1, \theta_2, \theta_3$ ) which can be written as:

$$\begin{aligned} &g^{III} \{\theta_1(\omega), \theta_2(\omega), \theta_3(\omega)\} \\ &= \left\{ \begin{array}{l} \psi^1(\theta_{1(1)} \dots \theta_{1(l)}), \psi^2(\theta_{2(1)} \dots \theta_{2(l)}), \psi^3(\theta_{3(1)} \dots \theta_{3(l)}) \end{array} \right\} \end{aligned}$$

(4) Compound effect of varying all properties ( $E_1, E_2, G_{12}, G_{23}, \nu_{12}, \nu_{23}, X_T, Y_T, S_{12}, G_{m1}, G_{f1}, \theta_1, \theta_2, \theta_3$ ) which can be written as:

$$\begin{aligned} &g^{IV} \{E_1(\omega), E_2(\omega), G_{12}(\omega), G_{23}(\omega), \nu_{12}(\omega), \nu_{23}(\omega), X_T(\omega), Y_T(\omega), S_{12}(\omega), \\ &G_{m1}(\omega), G_{f1}(\omega), \theta_1(\omega), \theta_2(\omega), \theta_3(\omega)\} \\ &= \left\{ \begin{array}{l} \psi^1(E_{1(1)} \dots E_{1(l)}), \psi^2(E_{2(1)} \dots E_{2(l)}), \psi^3(G_{12(1)} \dots G_{12(l)}), \\ \psi^4(G_{23(1)} \dots G_{23(l)}), \\ \psi^5(\nu_{12(1)} \dots \nu_{12(l)}), \psi^6(\nu_{23(1)} \dots \nu_{23(l)}), \psi^7(X_{T(1)} \dots X_{T(l)}), \\ \psi^8(Y_{T(1)} \dots Y_{T(l)}), \\ \psi^9(G_{m1(1)} \dots G_{m1(l)}), \psi^{10}(G_{f1(1)} \dots G_{f1(l)}), \psi^{11}(S_{12(1)} \dots S_{12(l)}), \\ \psi^{12}(\theta_{1(1)} \dots \theta_{1(l)}), \\ \psi^{13}(\theta_{2(1)} \dots \theta_{2(l)}), \psi^{14}(\theta_{3(1)} \dots \theta_{3(l)}) \end{array} \right\} \end{aligned}$$

Operator  $\psi$  generates the set of input parameters for performing Monte Carlo simulations.  $E_{1(i)}, E_{2(i)}, G_{12(i)}, G_{23(i)}, \nu_{12(i)}, \nu_{23(i)}, X_{T(i)}, Y_{T(i)}, S_{12(i)}, G_{m1(i)}, G_{f1(i)}$  and  $\theta_{1(i)}, \theta_{2(i)}, \theta_{3(i)}$  are material properties and ply orientations respectively, for  $i$ th sample. Symbol  $l$  denotes the total number of samples in Monte Carlo simulations. We have used  $\omega$  to represent the stochastic character of the respective parameters.

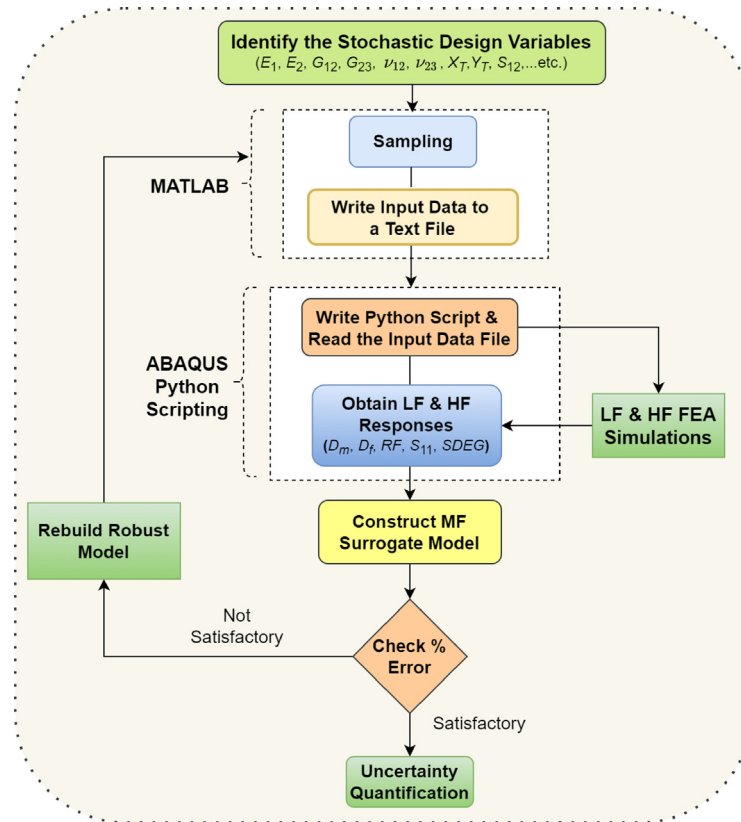


Fig. 4. Flow chart of the proposed multi-fidelity surrogate modelling approach for uncertainty quantification.

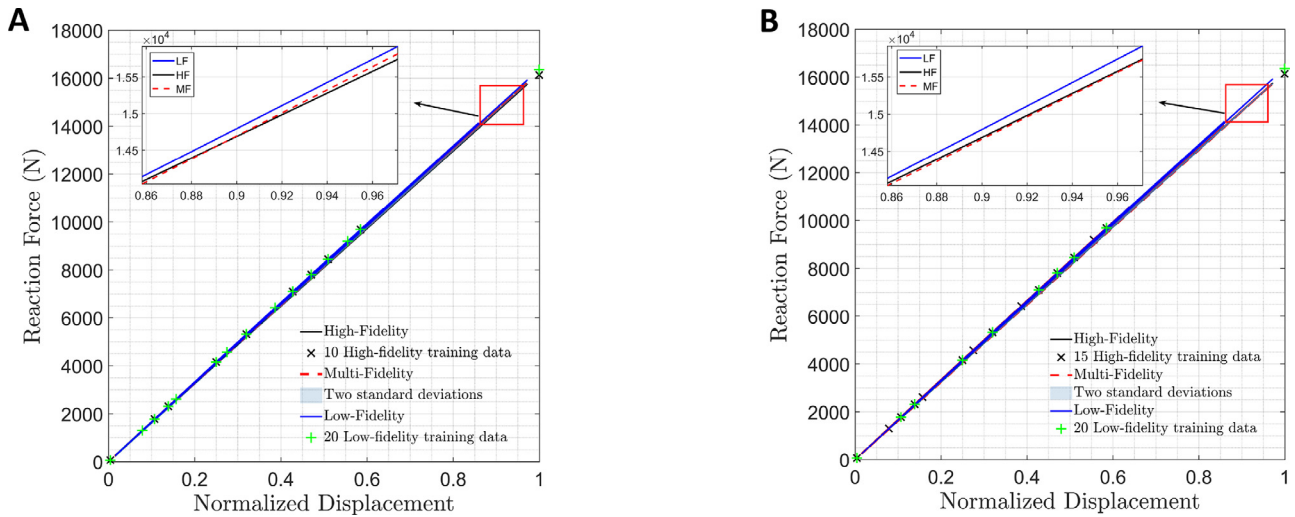


Fig. 5. Reaction force vs. displacement plots. (A) Reaction force vs. displacement plot using one-dimensional MF surrogate model comparing MF predictions (for 20 LF and 10 HF training samples) with LF and HF FEA simulation data. (B) Reaction force vs. displacement plot using one-dimensional MF surrogate model comparing MF predictions (for 20 LF and 15 HF training samples) with LF and HF FEA simulation data.

#### 4. Variance-based global sensitivity analysis

Global sensitivity analysis classifies the relative importance of uncertain input parameters based on the variance of the uncertain output (Trinh et al., 2020; Sinha and Mukhopadhyay, 2022; Bhowmik et al., 2022). First-order sensitivity indices represent the fractional contributions of uncertain inputs in the variance of the output while total sensitivity indices represent the sum of the main effects of uncertain parameters and all interactions in which those parameters are involved. The method proposed by Saltelli and Andrea (Saltelli,

2002) is adopted here for the computation of the sensitivity indices. The algorithm involved in the sensitivity analysis is discussed in the following paragraph.

Given that  $N$  is the number of evaluations, we obtain two  $(N, k)$  matrices called  $A$  and  $B$  using the Latin hypercube sampling method for the  $k$  dimensional model. We define a matrix  $C_i$ , which has all columns of the matrix  $B$  except  $i$ th column that has been taken from matrix  $A$ . Taking input from  $A$ ,  $B$  and  $C_i$  matrices, we get three outputs  $(N, 1)$ , as given in Saltelli et al. (2008).

$$\bar{y}_A = f(A), \quad \bar{y}_B = f(B), \quad \bar{y}_{C_i} = f(C_i) \quad (22)$$

**Table 5**

Percentage relative L2 norm error for one-dimensional HF and MF surrogate models. Here % error comparison is presented between the HF surrogate model trained with 30 and 50 HF data and the MF surrogate model trained with three sets of LF and HF data.

Surrogate model	Training samples	% relative L2 norm error				
		$RF$	$D_m$	$D_f$	$S_{11}$	$S_{DEG}$
High-fidelity	50 HF	0.003687	1.2092	1.7208	2.9377	0.3917
	30 HF	0.01130	1.17078	3.9238	2.9846	0.836123
Multi-fidelity	20 LF + 30 HF	0.009487	0.5567	1.3732	0.8242	0.5100
	20 LF + 20 HF	0.10	0.6284	3.2200	0.8333	4.1652
	20 LF + 10 HF	0.5286	2.6856	10.4172	3.5434	19.6162

**Table 6**

Comparison of computational time for training the HF and MF surrogate models for different sample sizes for one-dimensional case. The proportions of low and high fidelity training data and the corresponding accuracy of these samples are shown in Table 5. The computation time shown here is the time taken by finite element model for simulating the low and high-fidelity progressive damage in addition to surrogate model formation (computation time for training the multi-fidelity surrogates is comparatively negligible).

Sample size	HF computation time (Min)	MF computation time (Min)
30	180	150
40	230	215
50	300	270

The first-order indices are calculated as (Saltelli et al., 2008)

$$S_i = \frac{Var[E(Y|X_i)]}{Var(Y)} = \frac{\bar{y}_A \cdot \bar{y}_{C_i} - \bar{f}^2}{\bar{y}_A \cdot \bar{y}_A - \bar{f}^2} = \frac{(1/N) \sum_{j=1}^N \bar{y}_A^{(j)} \bar{y}_{C_i}^{(j)} - \bar{f}^2}{(1/N) \sum_{j=1}^N (\bar{y}_A^{(j)})^2 - \bar{f}^2} \quad (23)$$

where

$$\bar{f}^2 = \left( \frac{1}{N} \sum_{j=1}^N \bar{y}_A^{(j)} \right)^2$$

The total effects are calculated as

$$S_i^T = 1 - \frac{Var[E(Y|X_{\sim i})]}{Var(Y)} = 1 - \frac{\bar{y}_A \cdot \bar{y}_{C_i} - \bar{f}^2}{\bar{y}_A \cdot \bar{y}_A - \bar{f}^2} = 1 - \frac{(1/N) \sum_{j=1}^N \bar{y}_A^{(j)} \bar{y}_{C_i}^{(j)} - \bar{f}^2}{(1/N) \sum_{j=1}^N (\bar{y}_A^{(j)})^2 - \bar{f}^2} \quad (24)$$

The notation  $X_{\sim i}$  denotes the set of all variables except  $X_i$ . The total computational cost in this approach is  $N(k+2)$  runs instead of  $N^2$  runs of the brute-force method giving a computational advantage.

## 5. Uncertainty quantification: Results and discussion

In this section, we use the multi-fidelity surrogate-based approach (as described in Section 3) for the uncertainty quantification and global sensitivity analysis concerning reaction force, matrix damage, fibre damage, stress and delamination in AS4/PEEK  $([0/45/90/-45])_{2S}$  laminated composite under uniaxial tension in the longitudinal direction (refer to Fig. 1). The composite laminate has the following dimensions: length = 100 mm, width = 20 mm, and a circular hole at the centre with a diameter of 5 mm. The fibre damage contour plot in  $0^\circ$  ply and the matrix damage contour plots in  $0^\circ$ ,  $45^\circ$ ,  $90^\circ$  and  $-45^\circ$  plies are presented in Fig. 2 for the deterministic FEA model. It can be noted in this context that the current study involves a two-fold validation. Validation and convergence study of the finite element model has already been presented in Fig. 3, while the prediction accuracy and validation of the multi-fidelity surrogate models are discussed in this section. After having adequate confidence based on such two-fold validation, we have carried out uncertainty quantification and sensitivity analysis by exploiting the efficient surrogates of original simulation models. The flow chart of the proposed multi-fidelity surrogate modelling approach for uncertainty quantification is presented in Fig. 4. Note that a convergence study concerning the training sample size for surrogate formation is involved here. The multi-fidelity surrogate model is rebuilt with higher training sample size if the prediction error is not acceptable.

Once the surrogate prediction is accurate enough and acceptable for further analyses, the ‘rebuild’ step is not used any further.

Two problems (with one-dimensional and fifteen-dimensional input parameter space) have been taken for the demonstration of MF surrogate predictions. In the one-dimensional problem, we have taken stochastic variation in applied displacements while for the fifteen-dimensional problem, variation is taken in the material properties, displacements and ply orientations. Training samples are generated from an optimal Sobol sequence algorithm (Mukhopadhyay, 2018). Abaqus/standard 2016 version with the following computer specification is used to run FEA simulations: Intel(R) Xeon(R) W-1290 CPU at 3.20 GHz processor speed and 64 GB RAM, wherein 8 cores are utilized in parallel computing for surrogate model construction. In the context of number of input parameters for surrogate model formation, the curse of dimensionality is an important issue. One of the ways to look at the curse of dimensionality is that when we keep on increasing the dimensions or features of the problem to improve the model accuracy, the model prediction accuracy might drop after a threshold dimension value. Another way to look at it is when we increase the dimension of the problem, the data required to train the surrogate model increases exponentially. The notion of low, medium or high dimensional space is rather relative, wherein the complexity and nonlinearity involved in the model are also closely interlinked with the curse of dimensionality. Note that considering the complexity of the model of composite laminates and their progressive failure analysis, we referred to the fifteen-dimensional space as high-dimensional. In the current progressive damage model, we have taken almost all major input parameters which affect the global response of the composite laminate and the progressive damage behaviour. In this context, dimensionality reduction methods can also be explored to alleviate the curse of dimensionality in future studies.

One-dimensional multi-fidelity predictions are shown in Figs. 5 and 6. Multi-fidelity predictions as compared to LF and HF FEA data are shown in Fig. 7 for the fifteen-dimensional case. A data set of 25 points for the one-dimensional case and 100 points for the fifteen-dimensional case are used outside the training set for checking the prediction ability. We have further evaluated the following relative L2 norm error (RL2N Error) which is used for cross-benchmark comparison.

$$RL2N \text{ Error} = \frac{\sqrt{\sum_{i=1}^N |y_{pred}^{(i)} - y_{FEA}^{(i)}|^2}}{\sqrt{\sum_{i=1}^N |y_{FEA}^{(i)}|^2}} \quad (25)$$

where  $N$  denotes number of test samples,  $y_{pred}^{(i)}$  is a vector of surrogate model predictions and  $y_{FEA}^{(i)}$  is a vector of FEA predictions. The results concerning RL2N Error are shown in Tables 5 and 7 for the one and fifteen dimensional cases, respectively. In this context, it can be noted that multi-fidelity surrogate modelling is a data fusion approach. However, this also gives the opportunity to minimize the computational expense by choosing the necessary combination of low and high-fidelity training datasets depending on the required level of accuracy (refer to Tables 5 and 7). For this reason, we have brought in the notion of ‘optimal’ computational expenses in the context of data fusion. In future studies, it is also possible to involve different optimization algorithms to decide the proportion of high and low fidelity datasets for achieving

**Table 7**

Percentage relative L2 norm error for HF and MF surrogate models (fifteen dimensional case). Here % error comparison is presented between the HF surrogate model trained with 400, 600 and 1000 HF data and the MF surrogate model trained with three sets of LF and HF data.

Surrogate model	Training samples	% relative L2 norm error				
		$R_F$	$D_m$	$D_f$	$S_{11}$	$S_{DEG}$
High-fidelity	1000 HF	0.3871	2.7657	9.0157	2.390	17.458
	600 HF	0.2208	2.924	11.77	2.4519	20.5197
	400 HF	0.2212	3.6230	14.0563	2.7154	27.9870
Multi-fidelity	400 LF + 600 HF	0.2218	3.015	11.811	2.6005	19.109
	200 LF + 400 HF	0.2228	3.1477	11.88	2.6826	19.89
	200 LF + 200 HF	0.3361	4.997	20.9157	3.37	22.75
	200 LF + 100 HF	0.6142	6.7217	24.872	6.89	31.31

**Table 8**

Comparison of computational time for training the HF and MF surrogate models for different sample sizes for fifteen-dimensional case. The proportions of low and high fidelity training data and the corresponding accuracy of these samples are shown in Table 7. The computation time shown here is the time taken by finite element model for simulating the low and high-fidelity progressive damage in addition to surrogate model formation (computation time for training the multi-fidelity surrogates is comparatively negligible).

Sample size	HF computation time (Min)	MF computation time (Min)
300	1800	1550
400	2600	2400
600	3900	3700
1000	6500	6100

**Table 9**

Percentage coefficient of Variation (% COV) in responses for  $\pm 10^\circ$  stochasticity in material properties and  $\pm 10^\circ$  stochasticity in ply orientations.

Response	Input parameters	% COV
Matrix damage	Elastic properties	0.9%
	Failure properties	0.8%
	Ply orientation	1.22%
	All properties	1.85%
Fibre damage	Elastic properties	7.28%
	Failure properties	5.23%
	Ply orientation	9.94%
	All properties	16.98%
Reaction force	Elastic properties	7.29%
	Failure properties	0.17%
	Ply orientation	8.64%
	All properties	11.24%

a target level of accuracy. While forming the surrogate models, we have checked  $R^2$  values (correlation coefficient) for low-fidelity, high-fidelity and multi-fidelity surrogate predictions considering the one and fifteen dimensional cases, wherein a good correlation is noticed (values  $\sim 1$ ).

The validity and advantage of MF surrogate models are presented by comparing MF predictions against LF and HF FEA data. Fig. 5 shows the deterministic prediction capability of the one-dimensional ML surrogates to capture the entire constitutive curve. We show that the prediction capability of MF surrogates is far superior to LF surrogates and comparable to that of HF surrogates without the addition of significant computational costs for training. For the one-dimensional model, the computational cost of training the HF surrogate (refer to Table 6) is 300 min which uses 50 HF samples for training whereas the computational cost of training the MF surrogate is 270 min which uses 20 LF and 30 HF samples for training. Table 8 shows the computational costs of fifteen-dimensional model. It is noted that the computational cost of training the HF surrogate is 3900 min which uses 600 HF samples for training whereas the computational cost of training the MF surrogate is 3700 min which uses 200 LF and 400 HF samples for training, making it more computationally efficient than HF surrogate. While an increase in HF training data improves the prediction capability of MF surrogates, the trade-off needs to be addressed based on engineering

judgment of required accuracy and computation intensiveness. For the one-dimensional case, we further present scatter plots for reaction force, matrix damage, fibre damage, stress  $S_{11}$  and delamination corresponding to different values of applied displacement within the analysis domain (refer to Fig. 6). For each sample, these outputs are the maximum values in the model. The results demonstrate that the prediction capability of MF surrogates is significantly better than LF finite element simulations (and any surrogate formed based on LF training data). The results of RL2N Error for the one-dimensional case, as presented in Table 5 further corroborate the prediction accuracy of MF surrogates.

For the fifteen-dimensional case, we present scatter plots for reaction force, matrix damage, fibre damage, stress  $S_{11}$  and delamination corresponding to different random combinations of the input parameters within the analysis domain (refer to Fig. 7). The results demonstrate that the prediction capability of MF surrogates is significantly better than LF finite element simulations (and any surrogate formed based on LF training data). Percentage relative L2 norm error comparing MF surrogate predictions with HF surrogate predictions for the fifteen-dimensional case are shown in Table 7. From the results, we observe that the accuracy of the MF surrogate model can be increased by increasing HF training samples. However, the trade-off needs to be addressed based on engineering judgment of required accuracy and computation intensiveness. In this context, it can be noted that the one-dimensional problem considered in the preceding paragraph is a subset of the fifteen-dimensional problem. Thus the MF surrogates considering the fifteen-dimensional input parameter space can also be utilized to predict the complete constitutive curve presented in Fig. 5 by setting the value of all the other input parameters except displacement to their respective deterministic values. Similarly, the variation of deterministic reaction force (or other response quantities of interest) with respect to any other input parameter can be investigated without carrying out any additional finite element simulations, as presented in Fig. 8.

Having established the superiority of MF surrogates in deterministic predictions, we now investigate the complete probabilistic descriptions and statistical characteristics for reaction force, matrix damage, fibre damage, stress  $S_{11}$  and delamination based on Monte Carlo simulation considering 10 000 realizations. Table 9 presents a statistical study which shows the effect of variation in material and geometrical properties with different combinations on the responses of the laminate. Four groups of the input parameters (refer to Section 3.3) are made for this purpose (elastic properties, failure properties, ply orientations, All properties). From this study, it is noticed that variation in ply orientations affects the matrix damage, fibre damage and reaction force most. A  $\pm 10^\circ$  variation in ply orientations only gives 1.22%, 9.94% and 8.64% coefficient of variation in the matrix damage, fibre damage and reaction force respectively. A combined stochastic variation of  $\pm 10\%$  in material properties and  $\pm 10^\circ$  in ply orientations lead to 1.85%, 16.98% and 11.24% coefficient of variation in the matrix damage, fibre damage and reaction force respectively.

From Fig. 9, it can be observed that probability density function plots (PDF) obtained using MF surrogate models match closely with the HF model. In HF surrogate models, 600 HF training samples are

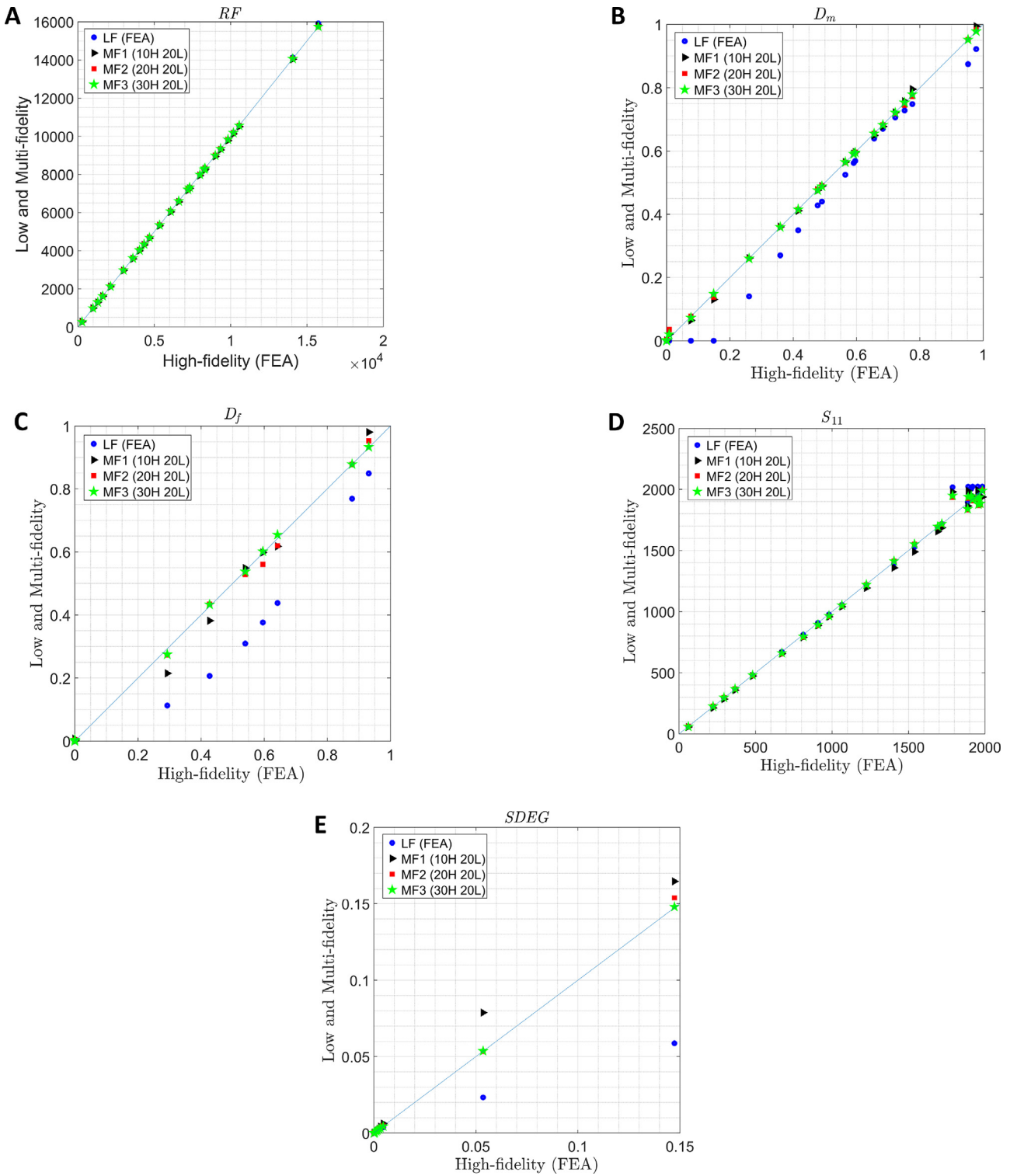


**Fig. 6. One-dimensional multi-fidelity scatter plots.** Scatter plots of the reaction force, the matrix damage, the fibre damage, the stress and the delamination obtained by MF surrogate models are presented with respect to LF and HF FEA simulation data. Three sets of LF and HF samples are used for training varying the applied displacement.

used for reaction force and 1000 training samples have been used for matrix damage, fibre damage, stress and delamination predictions while in the case of all multi-fidelity surrogate models, 200 LF and 400 HF training samples have been used, saving a fair amount of computational cost. After establishing the prediction ability of MF surrogates for deterministic and probabilistic computations, we present different individual and compound effects of stochasticity considering

the uncertainty cases described in Section 3.3. Fig. 10 presents the complete probabilistic descriptions for reaction force, matrix damage, fibre damage, stress  $S_{11}$  and delamination considering the individual effect of stochasticity in the elastic material properties, the failure properties, and ply orientation angles separately, along with the compound effect of stochasticity of all these input parameters (Refer to Section 3.3). The figure shows that the stochastic response bound and probabilistic

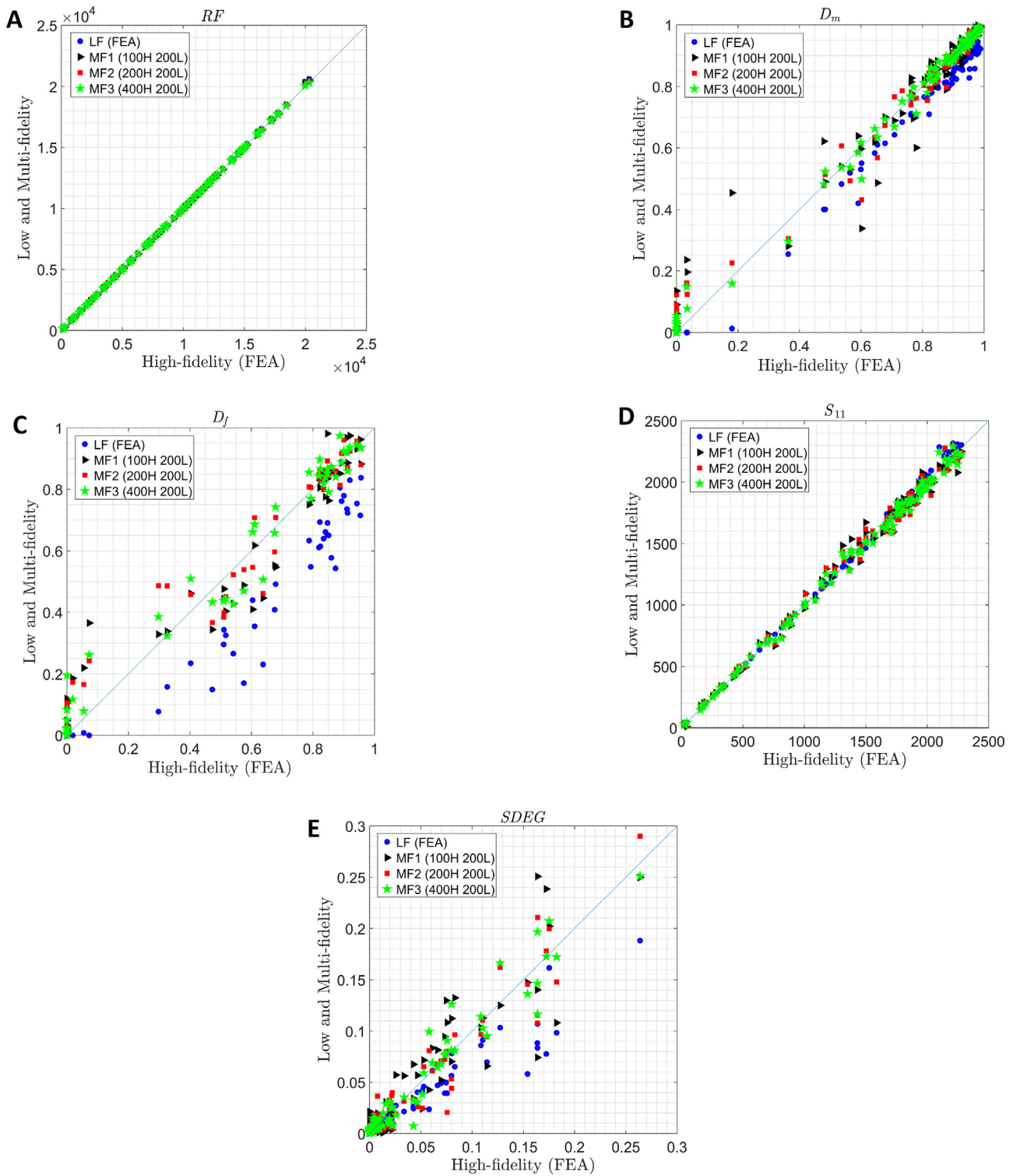


**Fig. 7. Fifteen-dimensional multi-fidelity scatter plots.** Scatter plots of the reaction force, the matrix damage, the fibre damage, the stress and the delamination obtained by MF surrogate models are presented with respect to LF and HF FEA simulation data. Three sets of LF and HF samples are used for training taking  $\pm 10\%$  stochasticity in material properties and  $\pm 10^\circ$  stochasticity in ply orientations.

distribution depend strongly on the nature of source-uncertainty under consideration. The compound effect of all the uncertain input parameters leads to the highest stochastic response bounds for all the output quantities of interest.

We have exploited the prediction capability of MF surrogates further to investigate the relative sensitivity of different input parameters.

A variance-based global sensitivity analysis (GSA) is presented here following Section 4, wherein the GSA indices are found to converge at 10000 samples. The results of GSA are presented in Fig. 11 considering different output quantities of interest. It is observed that  $0^\circ$  ply orientation, longitudinal elastic modulus ( $E_1$ ), in-plane Poisson's ratio ( $\nu_{12}$ ) and  $90^\circ$  ply orientation are the most sensitive (in descending

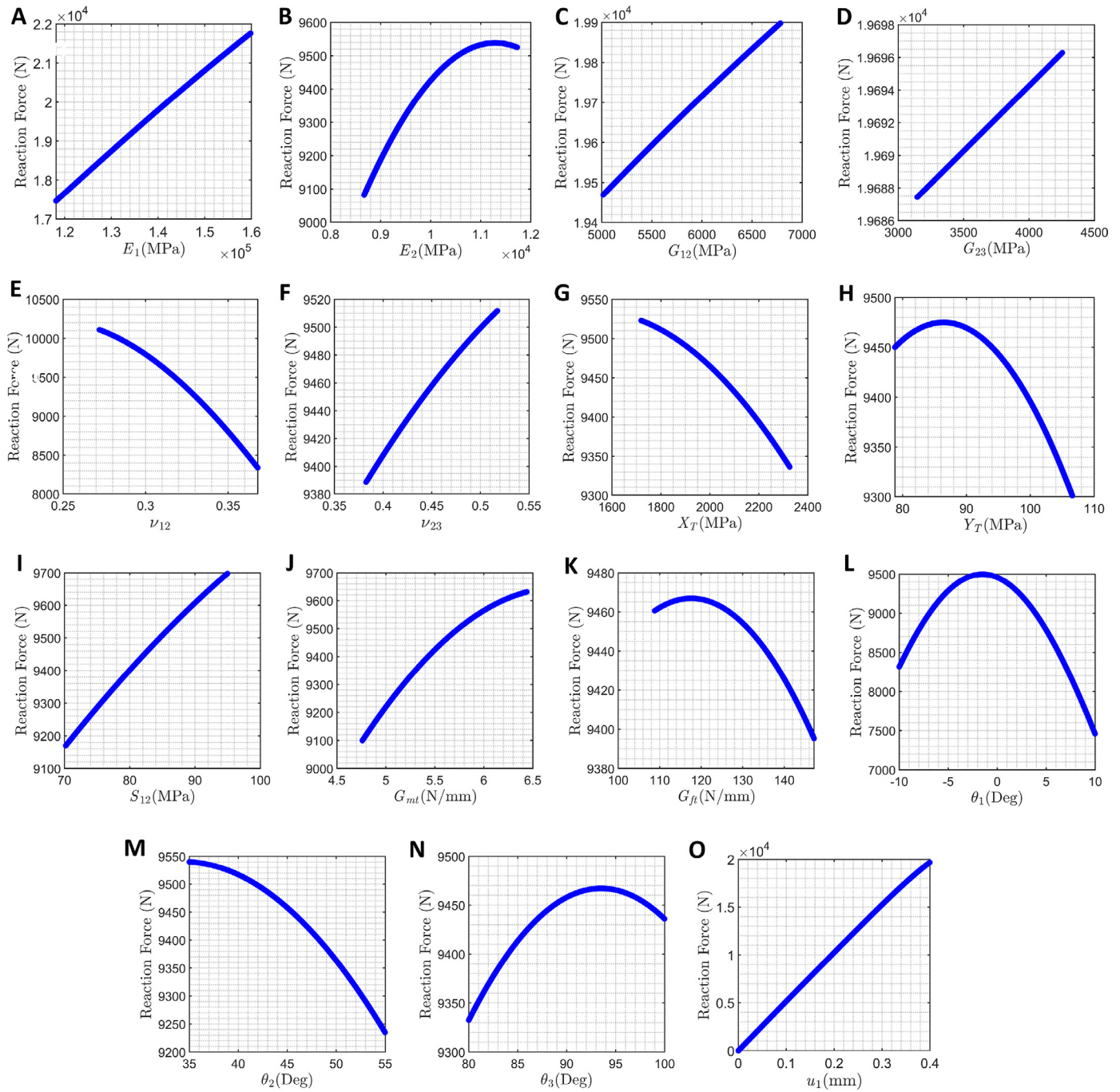


**Fig. 8. Deterministic variation of reaction force with respect to different influencing parameters individually.** (A–O) Influence of deterministic variation in input parameters on the reaction force. MF surrogates are used for the predictions. Here  $E_1$ ,  $G_{12}$ ,  $G_{23}$ ,  $E_2$ ,  $\nu_{12}$ ,  $\nu_{23}$ ,  $X_T$ ,  $Y_T$ ,  $S_{12}$ ,  $G_m$ ,  $G_f$ ,  $\theta_1$ ,  $\theta_2$ ,  $\theta_3$ ,  $u_1$  represents longitudinal elastic modulus, in-plane shear modulus, transverse shear modulus, transverse elastic modulus, in-plane Poisson's ratio, transverse Poisson's ratio, longitudinal tensile strength, transverse tensile strength, in-plane shear strength, matrix fracture energy in tension, fibre fracture energy in tension,  $0^\circ$  ply,  $45^\circ$  ply,  $90^\circ$  ply and applied displacement respectively.

order of sensitivity) while transverse Poisson's ratio ( $\nu_{23}$ ), transverse tensile strength ( $Y_T$ ), matrix fracture energy in tension ( $G_m$ ) are least sensitive input parameters to reaction force. The  $0^\circ$  ply orientation, applied displacement ( $u_1$ ), longitudinal elastic modulus ( $E_1$ ), in-plane Poisson's ratio ( $\nu_{12}$ ), ply orientation  $\theta_2$ , in-plane shear modulus ( $G_{12}$ ) and ply orientation  $\theta_3$  are the most sensitive (in descending order of sensitivity) parameters to matrix damage. For fibre damage,  $90^\circ$  ply orientation, longitudinal elastic modulus ( $E_1$ ), in-plane Poisson's ratio ( $\nu_{12}$ ), longitudinal tensile strength ( $X_T$ ), applied displacement ( $u_1$ ),  $45^\circ$  ply orientation and  $0^\circ$  ply orientation are the most sensitive (in

descending order of sensitivity) parameters. Applied displacement ( $u_1$ ) and longitudinal tensile strength ( $X_T$ ) are the only most sensitive input parameters to stress in the direction of applied load. Here parameter  $X_T$  is sensitive to the stress (which is the maximum stress in the laminate) is due to the fact that the maximum stress is dependent on the matrix and the fibre damage in the laminate and the matrix damage propagates in the laminate at much lower applied displacement than the nominal value of applied displacement 0.3 mm which is kept constant in the GSA. In case of delamination,  $90^\circ$  ply orientation,  $0^\circ$  ply orientation, in-plane Poisson's ratio ( $\nu_{12}$ ), longitudinal elastic modulus ( $E_1$ ), applied

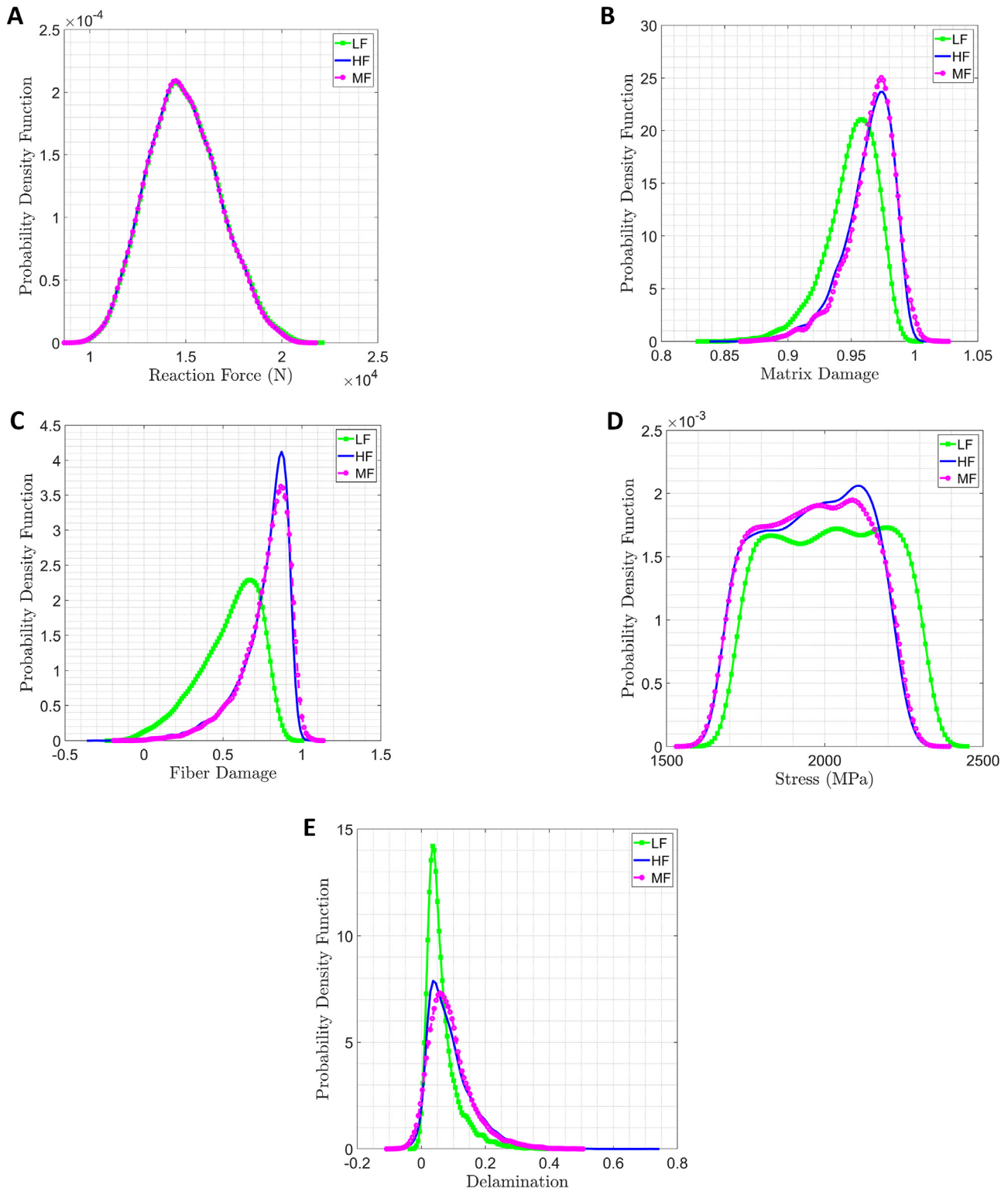


**Fig. 9. Probability density function (pdf) plots based on LF, HF and MF surrogate models.** Comparison among the pdfs of reaction force, matrix damage, fibre damage, stress and delamination obtained based on LF, HF and MF surrogate models (considering the compound effect of stochasticity). LF and MF surrogate models use 600 training samples for the prediction of the reaction force whereas 1000 training samples are used for the prediction of the fibre damage, the matrix damage, the stress and the delamination. 200 low-fidelity and 400 high-fidelity samples are used for the training of all MF surrogate models.

displacement ( $u_1$ ) and longitudinal tensile strength ( $X_T$ ) are most sensitive (in descending order of sensitivity) parameters. In-plane shear modulus does not affect the responses much except the matrix damage. It is also noted that ply orientations play a major role in the variation of

reaction force, matrix damage, fibre damage and delamination but not in the variation of stress. It may be noted that the first order and total sensitivity indices follow a similar trend (though the numerical values vary marginally) as presented in Fig. 11. An interesting correlation can

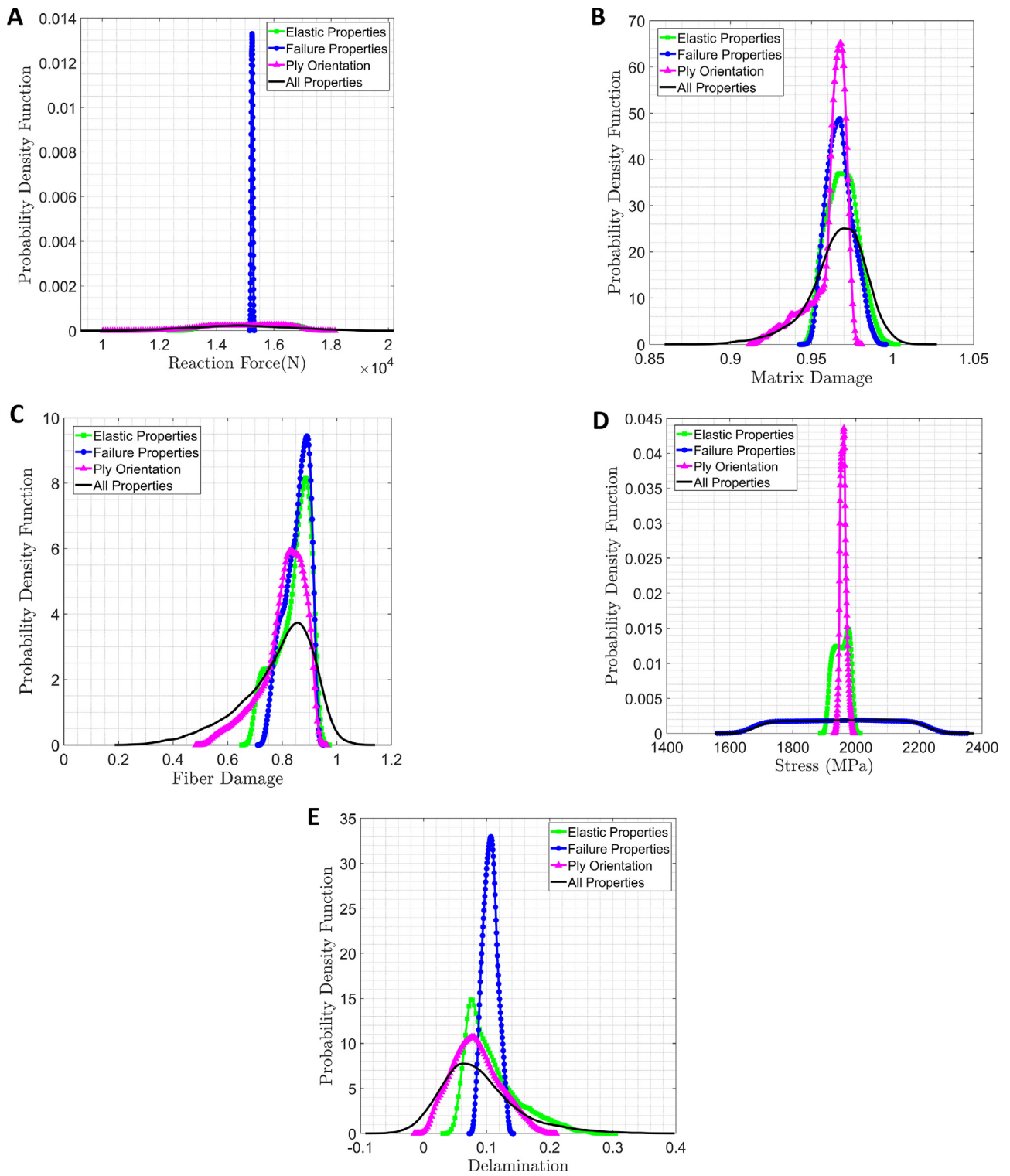


**Fig. 10.** Probability density function (pdf) plots representing individual and compound stochastic effects based on MF surrogate models. Comparison among the pdfs of reaction force, matrix damage, fibre damage, stress and the delamination obtained from multi-fidelity (MF) surrogate models is presented taking individual stochastic effects in elastic properties, failure properties, ply orientation and compound stochastic variation of all properties. 200 low-fidelity and 400 high-fidelity samples are used for the training of all MF surrogate models keeping the nominal applied displacement at 0.3 mm.

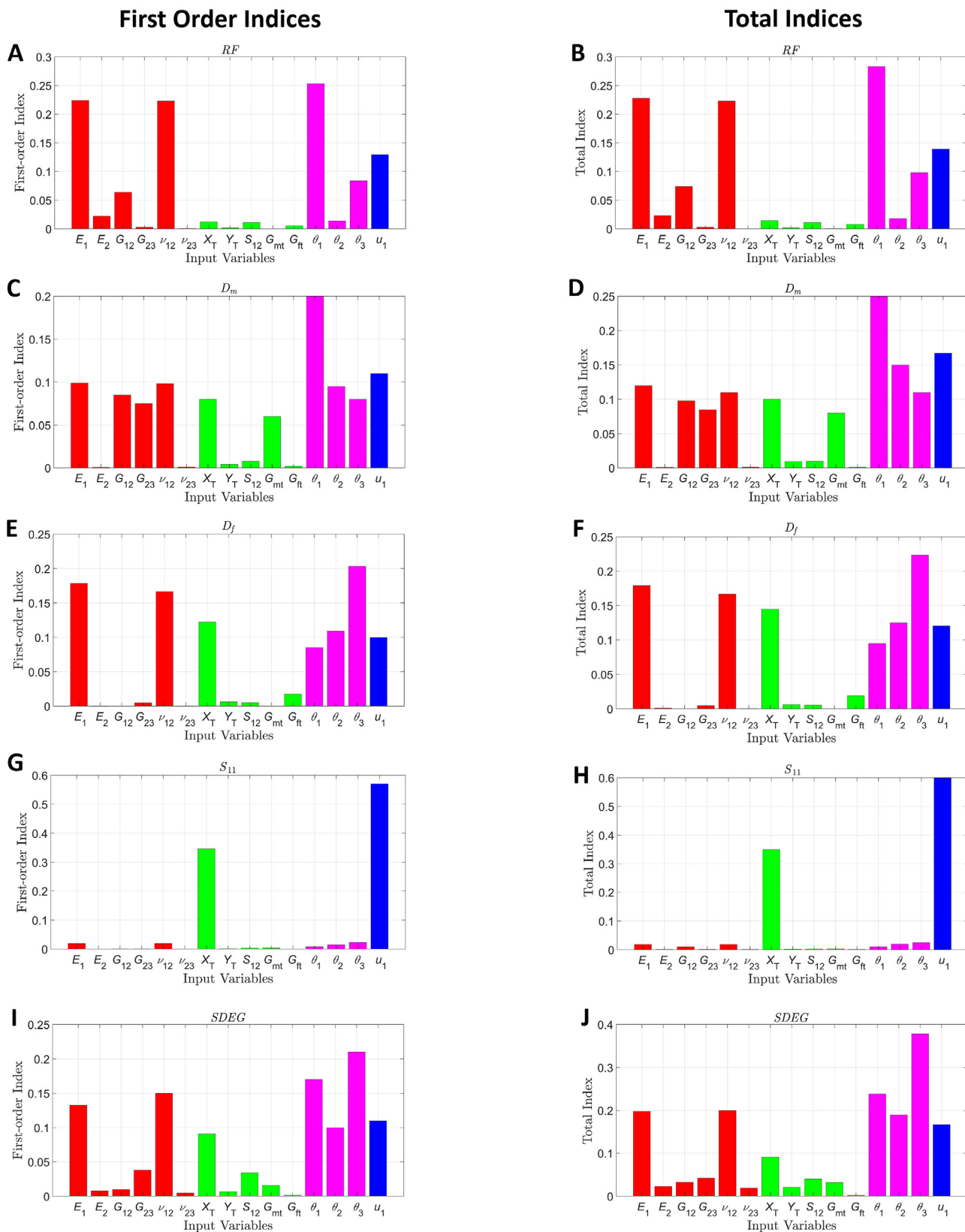


Fig. 11. Global sensitivity analysis. Variance-based global sensitivity analysis is carried out to understand the relative importance of the uncertain input parameters on reaction force, matrix damage, fibre damage, stress and delamination. (A, C, E, G, I) First-order sensitivity indices. (B, D, F, H, J) Total sensitivity indices.

be established between the sensitivity of different input parameters and the response bounds obtained considering different individual effects of stochasticity, as presented in Fig. 10.

## 6. Conclusions and perspective

An efficient stochastic progressive damage analysis framework is presented to quantify the uncertainty in notched composite laminates under uniaxial tension. A Gaussian process-based multi-fidelity (MF) machine learning algorithm is coupled with finite element simulations to train surrogate models for uncertainty quantification, wherein we combine low-fidelity (LF) finite element analysis data obtained using Matzenmiller damage model with Hasin failure criteria and high-fidelity (HF) finite element analysis data obtained using three-dimensional continuum mechanics based damage model with P Linde's failure criteria. The HF data used in MF surrogate model construction is much lesser as compared to that of HF surrogate models, resulting in a fair amount of reduction in computational cost while ensuring a sufficient level of accuracy. The hybrid multi-fidelity machine learning models can be regarded here as the most efficient surrogate of the occurrence of progressive damage in composite laminates that unify high and low fidelity damage models through optimal data fusion.

The proposed multi-fidelity surrogate modelling approach for composites essentially addresses the concern of having a large high-fidelity training dataset for accurate prediction by introducing a hybrid dataset and optimal data fusion. Since laminated composites involve a large number of input parameters and the finite element simulation model for composites is exorbitantly expensive, the required number of training datasets and the computational intensiveness for conventional surrogate modelling becomes quite high. The multi-fidelity modelling approach proves to be a panacea for uncertainty quantification of laminated composites.

The inevitable source-uncertainty in material (such as elastic and failure properties) and geometrical (such as ply orientation angle) properties is propagated from the input level to the global response level through the efficient MF surrogates along with Monte Carlo simulations for quantifying the stochastic reaction force, matrix damage, fibre damage, stress and delamination. Complete probabilistic descriptions corresponding to different individual and compound cases of stochasticity are captured through the Monte Carlo simulations, wherein the function evaluations are performed by exploiting the MF surrogates. The new probabilistic insights obtained through extensive numerical results strongly suggest that source-uncertainty of composites significantly influences the progressive damage evolution and global mechanical behaviour, leading to the realization of the importance of adopting an inclusive analysis framework considering such inevitable random variabilities. Further, computationally prohibitive global sensitivity analysis is performed based on the MF surrogate models to understand the relative significance of the uncertain input parameters on the critical responses. It is found that the ply orientations play the most important role in the variation of composite laminate damage, followed by different material properties depending on the response quantity of interest. Such sensitivity analysis can lead to significantly improved efficiency by incorporating only the sensitive parameters in the uncertainty modelling and selective quality control during design and manufacturing.

The novelty and impact of this article are two-fold: (1) quantifying the uncertainty associated with progressive failure of laminated composites, leading to complete probabilistic descriptions, along with sensitivity analysis, (2) developing the multi-fidelity ML based approach in conjunction with finite element simulations involving UMAT subroutine for efficient progressive damage analysis through optimal data fusion. Note that such multi-fidelity data fusion is attempted for the first time in this article involving the high dimensional stochastic parameter space of laminated composites for subsequent uncertainty quantification. It is particularly crucial for intensive stochastic sim-

ulations like progressive failure analysis of composites that require thousands of random realizations for the complete probabilistic characterization and prospective optimal designs including the effect of uncertain manufacturing effects. Thus the primary contribution of this article lies in coupling multi-fidelity machine learning models with optimal fusion of two different finite element based damage models of variable fidelity and computational intensiveness (Matzenmiller damage model with Hasin failure criteria and three-dimensional continuum mechanics based damage model with P Linde's failure criteria) for most efficient stochastic analysis of the progressive damage in composite laminates. This approach allows us to strike the desired balance in maximizing the accuracy while minimizing the computational expense. Other failure criteria and damage models can be integrated into this framework further depending on the problem under consideration. In general, the proposed multi-fidelity approach for uncertainty quantification here can be extended to dynamic and stability analysis, optimization and reliability analysis of laminated composites. In this work, we have propagated the inherent randomness (aleatoric uncertainty) in input parameters and quantified its effect on the progressive damage of composite laminates. Such variations in material and geometric attributes are normally quite significant due to manufacturing inaccuracies and service-life degradation. This work does not include epistemic uncertainty (lack of information in the system) in LF, HF and surrogate models. However, epistemic uncertainty involved in the Gaussian process models may be addressed in future works by quantifying it separately and superimposing it subsequently with the bounds of aleatoric uncertainty.

## CRedit authorship contribution statement

**R.S. Chahar:** Carried out the simulations, Prepared the results. **T. Mukhopadhyay:** Conceived the idea, analysis of results, writing the manuscript, supervision.

## Declaration of competing interest

The authors declare that they have no known competing financial interests or personal relationships that could have appeared to influence the work reported in this paper.

## Data availability

Data will be made available on request.

## Acknowledgements

RSC acknowledges the financial support received through a doctoral scholarship from IIT Kanpur during the research work. TM would like to acknowledge the research support received from the University of Southampton, United Kingdom.

## References

- Ansari, M.M., Chakrabarti, A., 2016. Progressive damage of GFRP composite plate under ballistic impact: experimental and numerical study. *Polym. Polym. Compos.* 24 (7), 579–586.
- Balokas, G., Kriegesmann, B., Czichon, S., Rolfes, R., 2021a. A variable-fidelity hybrid surrogate approach for quantifying uncertainties in the nonlinear response of braided composites. *Comput. Methods Appl. Mech. Engrg.* 381, 113851.
- Balokas, G., Kriegesmann, B., Rolfes, R., 2021b. Data-driven inverse uncertainty quantification in the transverse tensile response of carbon fiber reinforced composites. *Compos. Sci. Technol.* 211, 108845.
- Bhowmik, K., Mukhopadhyay, T., Tarfaoui, M., Khutia, N., Roy Chowdhury, A., Lafdi, K., 2022. Damage modeling of MWCNT reinforced carbon/epoxy composite using different failure criteria: a comparative study. *Appl. Phys. A* 128 (7), 1–22.
- Bostanabad, R., Liang, B., Gao, J., Liu, W.K., Cao, J., Zeng, D., Su, X., Xu, H., Li, Y., Chen, W., 2018. Uncertainty quantification in multiscale simulation of woven fiber composites. *Comput. Methods Appl. Mech. Engrg.* 338, 506–532.

- Camanho, P.P., Davila, C.G., De Moura, M., 2003. Numerical simulation of mixed-mode progressive delamination in composite materials. *J. Compos. Mater.* 37 (16), 1415–1438.
- Chen, J., Morozov, E., Shankar, K., 2012. A combined elastoplastic damage model for progressive failure analysis of composite materials and structures. *Compos. Struct.* 94 (12), 3478–3489.
- Chen, J.-F., Morozov, E.V., Shankar, K., 2014. Progressive failure analysis of perforated aluminium/CFRP fibre metal laminates using a combined elastoplastic damage model and including delamination effects. *Compos. Struct.* 114, 64–79.
- Dey, S., Mukhopadhyay, T., Adhikari, S., 2018. *Uncertainty Quantification in Laminated Composites: A Meta-Model Based Approach*. CRC Press.
- Dey, S., Mukhopadhyay, T., Khodaparast, H.H., Adhikari, S., 2016a. A response surface modelling approach for resonance driven reliability based optimization of composite shells. *Periodica Polytech. Civ. Eng.* 60 (1), 103–111.
- Dey, S., Mukhopadhyay, T., Spickenheuer, A., Adhikari, S., Heinrich, G., 2016b. Bottom up surrogate based approach for stochastic frequency response analysis of laminated composite plates. *Compos. Struct.* 140, 712–727.
- Forrester, A.I., Söbester, A., Keane, A.J., 2007. Multi-fidelity optimization via surrogate modelling. *Proc. R. Soc. Lond. Ser. A Math. Phys. Eng. Sci.* 463 (2088), 3251–3269.
- Gao, G., An, L., Giannopoulos, I.K., Han, N., Ge, E., Hu, G., 2020. Progressive damage numerical modelling and simulation of aircraft composite bolted joints bearing response. *Materials* 13 (24), 5606.
- Ghannadpour, S., Kurkaani Barvaj, A., Tornabene, F., 2018. A semi-analytical investigation on geometric nonlinear and progressive damage behavior of relatively thick laminated plates under lateral pressure and end-shortening. *Compos. Struct.* 194, 598–610.
- Guo, Q., Hang, J., Wang, S., Hui, W., Xie, Z., 2020. Buckling optimization of variable stiffness composite cylinders by using multi-fidelity surrogate models. *Thin-Walled Struct.* 156, 107014.
- Hashin, Z., 1980. Failure criteria for unidirectional fiber composites.
- Hinton, M., Kaddour, A., Soden, P., 2002. A comparison of the predictive capabilities of current failure theories for composite laminates, judged against experimental evidence. *Compos. Sci. Technol.* 62 (12–13), 1725–1797.
- Hosseinpour, M., Daei, M., Zeynalian, M., Ataei, A., 2023. Neural networks-based formulation for predicting ultimate strength of bolted shear connectors in composite cold-formed steel beams. *Eng. Appl. Artif. Intell.* 118, 105614.
- Karsh, P., Mukhopadhyay, T., Dey, S., 2018. Spatial vulnerability analysis for the first ply failure strength of composite laminates including effect of delamination. *Compos. Struct.* 184, 554–567.
- Krishnan, K.V., Ganguli, R., 2021. Multi-fidelity analysis and uncertainty quantification of beam vibration using co-kriging interpolation method. *Appl. Math. Comput.* 398, 125987.
- Lapczyk, I., Hurtado, J.A., 2007. Progressive damage modeling in fiber-reinforced materials. *Composites A* 38 (11), 2333–2341.
- Lin, Q., Zhou, Q., Hu, J., Cheng, Y., Hu, Z., 2022. A sequential sampling approach for multi-fidelity surrogate modeling-based robust design optimization. *J. Mech. Des.* 144 (11), 111703.
- Linde, P., Pleitner, J., de Boer, H., Carmone, C., 2004. Modelling and simulation of fibre metal laminates. In: *ABAQUS Users' Conference*, Vol. 421.
- Liu, X., Tao, F., Yu, W., 2020. A neural network enhanced system for learning nonlinear constitutive law and failure initiation criterion of composites using indirectly measurable data. *Compos. Struct.* 252, 112658.
- Maa, R.-H., Cheng, J.-H., 2002. A CDM-based failure model for predicting strength of notched composite laminates. *Composites B* 33 (6), 479–489.
- Maimí, P., Camanho, P.P., Mayugo, J., Dávila, C., 2007. A continuum damage model for composite laminates: Part II—computational implementation and validation. *Mech. Mater.* 39 (10), 909–919.
- Mandal, B., Chakrabarti, A., 2018. Elasto-plastic damage model considering cohesive matrix interface layers for composite laminates. *J. Mech. Sci. Technol.* 32 (1), 121–127.
- Matzenmiller, A., Lubliner, J., Taylor, R.L., 1995. A constitutive model for anisotropic damage in fiber-composites. *Mech. Mater.* 20 (2), 125–152.
- Mukhopadhyay, T., 2018. A multivariate adaptive regression splines based damage identification methodology for web core composite bridges including the effect of noise. *J. Sandw. Struct. Mater.* 20 (7), 885–903.
- Mukhopadhyay, T., Naskar, S., Chakraborty, S., Karsh, P., Choudhury, R., Dey, S., 2021. Stochastic oblique impact on composite laminates: a concise review and characterization of the essence of hybrid machine learning algorithms. *Arch. Comput. Methods Eng.* 28, 1731–1760.
- Mukhopadhyay, T., Naskar, S., Karsh, P., Dey, S., You, Z., 2018. Effect of delamination on the stochastic natural frequencies of composite laminates. *Composites B* 154, 242–256.
- Naskar, S., Mukhopadhyay, T., Sriramula, S., 2018. Probabilistic micromechanical spatial variability quantification in laminated composites. *Composites B* 151, 291–325.
- Naskar, S., Mukhopadhyay, T., Sriramula, S., 2019. Spatially varying fuzzy multi-scale uncertainty propagation in unidirectional fibre reinforced composites. *Compos. Struct.* 209, 940–967.
- Pagani, A., Petrolo, M., Sánchez-Majano, A., 2023. Stochastic characterization of multiscale material uncertainties on the fibre-matrix interface stress state of composite variable stiffness plates. *Internat. J. Engng. Sci.* 183, 103787.
- Raissi, M., Karniadakis, G., 2016. Deep multi-fidelity Gaussian processes. *arXiv preprint arXiv:1604.07484*.
- Raissi, M., Perdikaris, P., Karniadakis, G.E., 2017. Inferring solutions of differential equations using noisy multi-fidelity data. *J. Comput. Phys.* 335, 736–746.
- Saltelli, A., 2002. Making best use of model evaluations to compute sensitivity indices. *Comput. Phys. Comm.* 145 (2), 280–297.
- Saltelli, A., Ratto, M., Andres, T., Campolongo, F., Cariboni, J., Gatelli, D., Saisana, M., Tarantola, S., 2008. *Global Sensitivity Analysis: the Primer*. John Wiley & Sons.
- Sharma, A.P., Khan, S.H., Parameswaran, V., 2017. Experimental and numerical investigation on the uni-axial tensile response and failure of fiber metal laminates. *Composites B* 125, 259–274.
- Sharma, A., Mukhopadhyay, T., Kushvaha, V., 2022a. Experimental data-driven uncertainty quantification for the dynamic fracture toughness of particulate polymer composites. *Eng. Fract. Mech.* 273, 108724.
- Sharma, A., Mukhopadhyay, T., Rangappa, S.M., Siengchin, S., Kushvaha, V., 2022b. Advances in computational intelligence of polymer composite materials: machine learning assisted modeling, analysis and design. *Arch. Comput. Methods Eng.* 29 (5), 3341–3385.
- Sinha, P., Mukhopadhyay, T., 2022. Effective elastic properties of lattice materials with intrinsic stresses. *Thin-Walled Struct.* 173, 108950.
- Smith, M., 2009. *ABAQUS/Standard User's Manual, Version 6.9*. Dassault Systèmes Simulia Corp, United States.
- Sriramula, S., Chryssanthopoulos, M.K., 2009. Quantification of uncertainty modelling in stochastic analysis of FRP composites. *Composites A* 40 (11), 1673–1684.
- Tao, F., Liu, X., Du, H., Yu, W., 2021. Learning composite constitutive laws via coupling abaqus and deep neural network. *Compos. Struct.* 272, 114137.
- Tao, W., Zhu, P., Xu, C., Liu, Z., 2020. Uncertainty quantification of mechanical properties for three-dimensional orthogonal woven composites. Part II: Multiscale simulation. *Compos. Struct.* 235, 111764.
- Thapa, M., Paudel, A., Mulani, S.B., Walters, R.W., 2021. Uncertainty quantification and global sensitivity analysis for progressive failure of fiber-reinforced composites. *Struct. Multidiscip. Optim.* 63 (1), 245–265.
- Tian, K., Li, Z., Zhang, J., Huang, L., Wang, B., 2021. Transfer learning based variable-fidelity surrogate model for shell buckling prediction. *Compos. Struct.* 273, 114285.
- Tornabene, F., Fantuzzi, N., Baccocchi, M., Viola, E., 2018. Mechanical behavior of damaged laminated composites plates and shells: Higher-order shear deformation theories. *Compos. Struct.* 189, 304–329.
- Trinh, M.-C., Mukhopadhyay, T., Kim, S.-E., 2020. A semi-analytical stochastic buckling quantification of porous functionally graded plates. *Aerosp. Sci. Technol.* 105, 105928.
- Vaishali, Mukhopadhyay, T., Kumar, R., Dey, S., 2021. Probing the multi-physical probabilistic dynamics of a novel functional class of hybrid composite shells. *Compos. Struct.* 262, 113294.
- Vaishali, Mukhopadhyay, T., Naskar, S., Dey, S., 2023. On machine learning assisted data-driven bridging of FSDT and HOZT for high-fidelity uncertainty quantification of laminated composite and sandwich plates. *Compos. Struct.* 304, 116276.
- West IV, T.K., Phillips, B.D., 2020. Multifidelity uncertainty quantification of a commercial supersonic transport. *J. Aircr.* 57 (3), 491–500.
- Xu, Z., Gao, T., Li, Z., Bi, Q., Liu, X., Tian, K., 2023. Digital twin modeling method for hierarchical stiffened plate based on transfer learning. *Aerospace* 10 (1), 66.
- Yan, S., Zou, X., Ilkhani, M., Jones, A., 2020. An efficient multiscale surrogate modelling framework for composite materials considering progressive damage based on artificial neural networks. *Composites B* 194, 108014.
- Yoo, K., Bacarreza, O., Aliabadi, M.F., 2021. Multi-fidelity robust design optimisation for composite structures based on low-fidelity models using successive high-fidelity corrections. *Compos. Struct.* 259, 113477.